



Schweizerische Eidgenossenschaft
Confédération suisse
Confederazione Svizzera
Confederaziun svizra

Swiss Confederation

Eidgenössisches Nuklearsicherheitsinspektorat ENSI
Inspection fédérale de la sécurité nucléaire IFSN
Ispettorato federale della sicurezza nucleare IFSN
Swiss Federal Nuclear Safety Inspectorate ENSI



Verification of Nagra's Biosphere Modelling Results Project 'Opalinus Clay'

Expertenbericht

**AMPHOS21 Consulting S.L.
Barcelona (Spain)**

Mai 2012

Verification of Nagra's Biosphere Modelling Results

Project 'Opalinus Clay'

Alba Valls

Lara Duro

Expertenbericht zuhanden des
Eidgenössischen Nuklearsicherheitsinspektorates ENSI

May, 2012



Impressum

Publisher

Swiss Federal Nuclear Safety Inspectorate ENSI

Industriestrasse 19

CH-5200 Brugg

Phone: +41 (0)56 460 84 00

info@ensi.ch

Cover photograph: BAFU/Raffael Waldner

ENSI, May 2012



Table of Contents

1. INTRODUCTION.....	1
2. METHODOLOGY.....	3
3. SYSTEM DESCRIPTION.....	4
3.1 CONCEPTUAL MODEL.....	6
3.1.1 <i>Physical sub-model</i>	7
3.1.2 <i>Exposure pathway sub-model</i>	11
3.2 NUMERICAL MODEL.....	14
3.2.1 <i>Physical sub-model</i>	14
3.2.2 <i>Exposure pathway sub-model</i>	18
4. COMPARISON EXERCISE.....	31
5. SENSITIVITY ANALYSIS.....	35
5.1 SENSITIVITY TEST 1 (<i>EXPOSURE PATHWAY SUB-MODEL</i>).....	36
5.2 SENSITIVITY TEST 2 (<i>PHYSICAL SUB-MODEL</i>).....	39
6. CONTEXTUALIZATION OF THE MODEL WITH OTHER APPROACHES	49
6.1 SBK, SWEDEN	49
6.2 POSIVA, FINLAND.....	52
6.3 ANDRA, FRANCE.....	56
6.4 NIROND, BELGIUM	58
6.5 NWMO, CANADA.....	60
6.6 PAMINA, EUROPEAN PROJECT.....	63
6.7 BDCF COMPARISON.....	67
7. SUMMARY AND CONCLUSIONS.....	69
8. REFERENCES.....	72
APPENDIX A: DATA USED FOR REFERENCE CASE	74
A1. SPECIFIC RADIONUCLIDE DATA.....	74



A2. NON-RADIONUCLIDE DEPENDENT DATA USED IN PHYSICAL SUB-MODEL	75
A3. RADIONUCLIDE DEPENDENT DATA USED IN PHYSICAL SUB-MODEL	78
A4. NON-RADIONUCLIDE DEPENDENT DATA USED IN EXPOSURE PATHWAY SUB-MODEL.....	84
A5. RADIONUCLIDE DEPENDENT DATA USED IN EXPOSURE PATHWAY SUB-MODEL.....	86



1. Introduction

Nuclear wastes generated in Switzerland, both SF/HLW (spent fuel elements/high level waste) and LILW (low and intermediate level waste), are planned to be disposed in a geological repository.

The Swiss Sectoral Plan for Deep Geological Repositories envisages three phases for the site selection:

Stage 1: Selection of geological siting areas

Stage 2: Selection of at least two potential sites for SF/HLW and LILW repositories respectively

Stage 3: Site selection and general license procedure

The potential sites proposed as the result of stage 1 will be compared on the basis of radiation doses to individuals of the most exposed group, derived from a provisional assessment of long-term safety.

In the frame of the second stage, the Swiss Federal Nuclear Safety Inspectorate (ENSI) is in charge of the examination and review of submitted reports with respect to safety and technical feasibility. In view of this task, ENSI is seeking the assistance to develop their biosphere model capabilities.

The Swiss National Cooperative for the Disposal of Radioactive Waste (Nagra) is in charge of conducting the performance assessment of the nuclear waste repository. ENSI is in charge of reviewing Nagra's work and ensuring that it is done in accordance with Swiss regulations and with the required level of confidence. Part of the assessment involves the verification of the Biosphere Dose Conversion Factors (BDCF) derived by Nagra in the context of project 'Opalinus Clay'.

The objective of this work is the derivation of the Biosphere Dose Conversion Factors (BDCF) by using an alternative modeling tool and the study of how several simplifications incorporated to the model affect the results.



The present work constitutes the basis of an expanded study aiming at developing ENSI's biosphere modeling capabilities, including the selection of a suitable computer program for biosphere transport and dose calculations alternative to the one used by Nagra.

The present report is organised into six main sections:

Chapter 2 presents the methodology of the work;

Chapter 3 describes the system, conceptual and numerical model;

Chapter 4 compares the results of the BDCFs obtained with those reported by Nagra

Chapter 5 presents the results of two simplifications of the base model;

Chapter 6 gives the international context by comparing the model implemented with those followed by other nuclear waste management organisations;

Chapter 7 presents a brief summary and the main conclusions obtained from this work.

Specific data of interest used in the development of the model are given in Appendix A1 to A5, included at the end of the report.

2. Methodology

This project has been conducted in four steps (Figure 1):

- 1) *Model implementation*: conceptualization and parameterization of the model and implementation in the calculation code (section 3)
- 2) *BDCFs*: calculation of the BDCFs and their comparison with the ones obtained by Nagra in the frame of the 'Opalinus Clay' project (section 4)
- 3) *Simplifications*: tests to simplify the reference case of the 'Opalinus Clay' project and comparison with previous results (section 5)
- 4) *Comparison with other BDCF assessments*: comparison of the conceptual models and, when possible, comparison of the BDCFs obtained in the biosphere approaches elaborated by other national organizations (section 6)

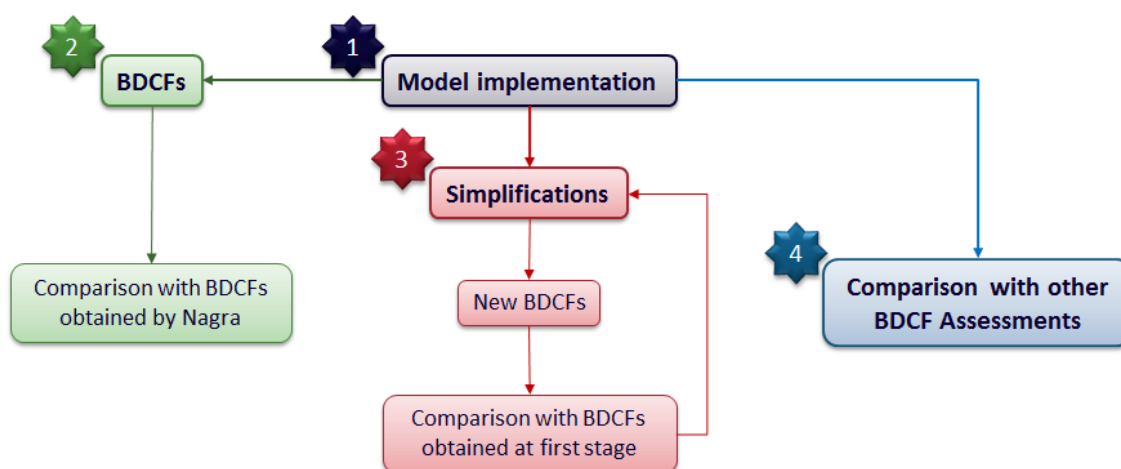


Figure 1. Scheme of the methodology followed in this report.

A more detailed description of the methodology is provided at the beginning of each section when required.

3. System description

The aim of this project is the verification of the Nagra's biosphere modelling developed in the frame of the 'Opalinus Clay' project. Therefore, the same system followed by Nagra for the post-closure radiological safety assessment of a deep geological repository is considered. The repository concept under study is sited in the Opalinus Clay of the Zürcher Weinland region (Northern Switzerland) and is designed for the disposal of spent nuclear fuel, vitrified high level wastes and long-lived intermediate level wastes (Nagra 2002a).

The safety assessment developed by Nagra deals with the complete system, from the waste itself to the release into the biosphere, resulting in the calculation of individual doses to human living in the affected area. The evaluation has been split into 3 submodels each of them calculated separately, as follows (Nagra 2002b):

- a. *Near field*: model used to evaluate the release of radionuclides from the waste and their transport through the engineered barrier system of the repository
- b. *Geosphere or Far field*: model used to evaluate the transport of radionuclides through the repository host rock and adjacent geological formations
- c. *Biosphere*: model used to evaluate the distribution of radionuclides in the surface environment and the exposure pathways that result in an individual dose

This project is focused on the third sub-model, the biosphere. The end point of the biosphere assessment is the calculation of BDCFs. Nagra assumes that the timescales of different phenomena resulting in the transfer of radionuclides to the biosphere are short in comparison with the timescales of the radionuclides release from the Opalinus Clay. Thus, BDCFs derived from the biosphere model will be multiplied by the releases from the geosphere into the biosphere to obtain the individual dose.

Eight scenarios are considered in the biosphere assessment performed by Nagra. BDCF comparison exercise is presented for the *Reference Case* scenario.

Biosphere Reference Case: general description

The present climate state is the base of the Reference Case conceptualization which considers the local geomorphological unit ‘eroding river’¹ (Figure 2). Contaminated groundwater from the geosphere is assumed to discharge into the Quaternary gravel aquifer in the Rhine valley (Nagra 2003).

Dilution of radionuclides in the aquifer occurs due to the upstream groundwater flow, lateral inflow from valley sides and precipitation. Contaminated groundwater reaches the top soil by irrigation and it is assumed that all water used by irrigation comes from the gravel aquifer of the studied area. Capillary rise is excluded because the distance between groundwater table and the rooting zone is too large.

Precipitation and evapotranspiration values (1 and 0.6 m/y, respectively) are selected as typical rates for the present climate in northern Switzerland. Erosion rate is assumed to compensate an uplift rate of 0.1 mm/y and sedimentation is not considered.

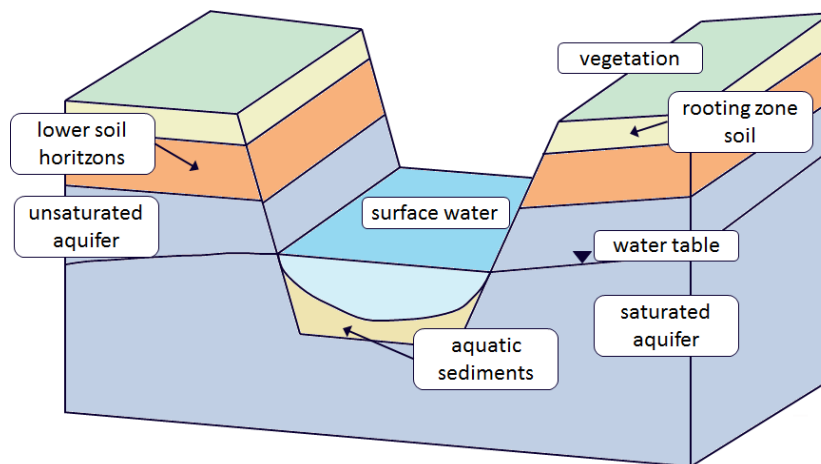


Figure 2: Scheme of the Reference Case biosphere system (adapted from Nagra 2003)

¹ Local geomorphic unit ‘eroding river’: Relatively narrow, cut-in river section where solid material balance is dominated by erosion (e.g. V-shaped valleys, gravel terraces). Eroding rivers cause linear erosion and act as regional base level for denudation (quotation from Nagra 2003).

All exposure pathways have been considered to calculate the dose received by one individual of the critical group which spends all time in the affected area. All food consumed is cultivated and raised in the area of study.

In the following sections, the conceptual model and its numerical representation are presented (section 3.1 and 3.2, respectively).

3.1 Conceptual model

The biosphere *Reference Case* system is conceptualized as a compartmental model (box model). The subsequent implementation is done in a computer program based on compartmental modelling calculations. Nagra used the code TAME to evaluate the dose conversion factors which are the main output of the biosphere assessment. In the present project, AMBER© is the selected program to perform the BDCF calculations. It is also a compartmental modelling code, which allows for an accurate reproduction of the model developed by Nagra.

The biosphere system is divided in two parts:

- the physical biosphere, and
- the exposure pathways.

The physical part describes the components of the surface environment (e.g. agricultural areas, lakes, rivers, aquifers, soils...) and the fluxes between them. Exposure pathways are determined, mainly, by the human behaviour (e.g. transfer of radionuclides through the food chain, diet habits, agricultural practices...).

The model development has the aim of obtaining the radiological impact of several radionuclides to human. In the present report the radionuclides considered of interest for the comparison exercise are: ^{14}C , ^{36}Cl , ^{79}Se , ^{129}I and the ^{246}Cm decay chain. This series includes four non-metallic elements (C, Cl, Se and I) and seven metallic ones derived from the ^{246}Cm decay chain (Cm, Pu, U, Th, Ra, Pb and Po). The selection of the Cm chain daughters is based on the half-life or radiological impact.

Figure 3 shows the decay chain of curium. The radionuclides considered in the present study are highlighted in green.

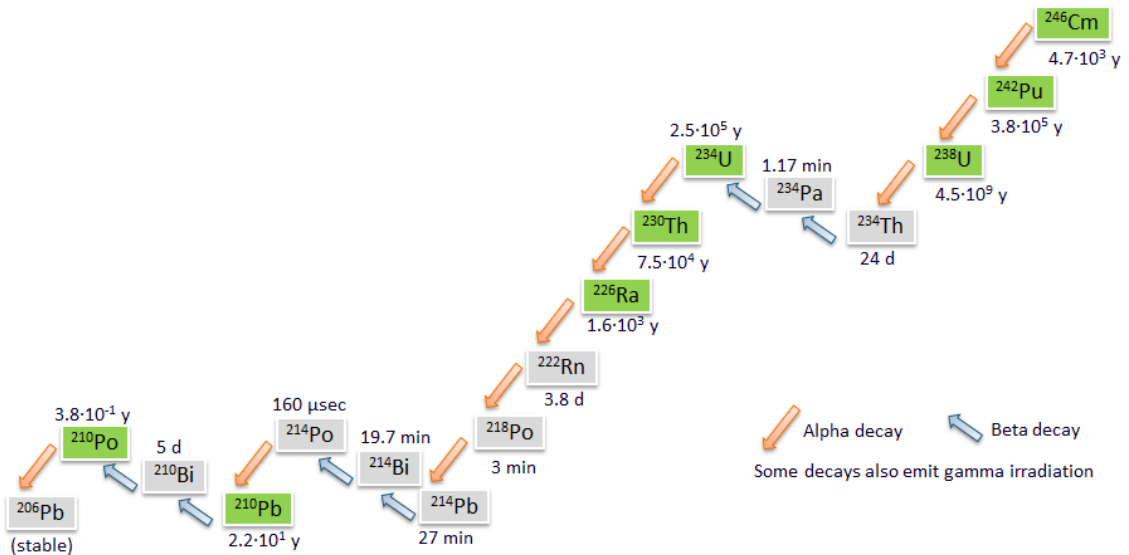


Figure 3: ^{246}Cm decay chain. Radionuclides included in this study are highlighted in green.

3.1.1 Physical sub-model

Five compartments are used to represent different biosphere media appearing in the scheme of Figure 2:

- local Quaternary aquifer (L),
- deep soil (D),
- top soil (T),
- surface water (river) (W) and
- bed sediments (B).

An additional compartment has been described that corresponds to a sink and it is called *Elsewhere* (E). Figure 4 shows all the compartments of the system and the transferences that are considered to occur between them.

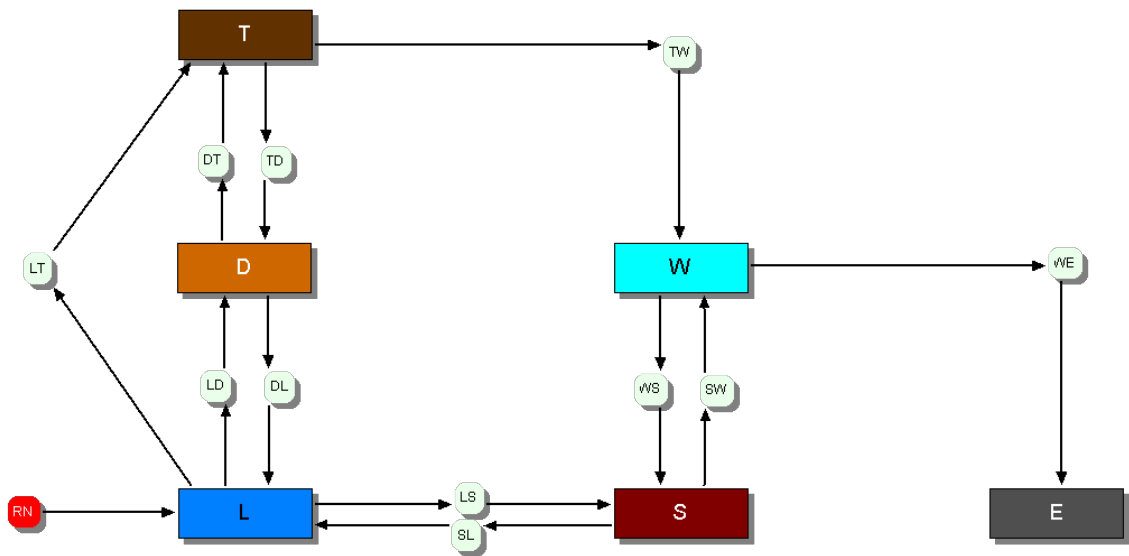


Figure 4: Reference Case model implemented in AMBER©. Boxes stand for compartments and arrows represent radionuclide transferences between compartments. Compartment abbreviations: T (Top soil), D (Deep soil), L (Local aquifer), S (bed Sediment), W (surface Water) and E (Elsewhere). Transfer names are chosen as XY where X is the letter representing the donor compartment and Y the one of the receptor compartment.

Radionuclides released from geosphere (red box called 'RN' in Figure 4) reach the biosphere system through the local aquifer. Their transport from this compartment to the rest of them (T, D, S, W, E) occurs as a result of the movement of water and diffusion, when radionuclides are in solution, and transfer of solid material in the case of radionuclides sorbed onto mobile solid phases. The mechanisms of radionuclide transport are detailed below.

Water fluxes (Figure 5)

Water from the geosphere discharges in three different biosphere compartments: top soil (precipitation), local aquifer (upstream groundwater) and surface water (upstream water flux).

The top soil also receives water from the local aquifer, through irrigation of crops and pastures. Water from the top soil infiltrates to the deep soil.

Water of the local aquifer is also flowing to bed sediments and, reaches the surface water compartment. The outflows of the system occur by evapotranspiration in the top soil compartment and by water flow from the river flowing in the studied area.

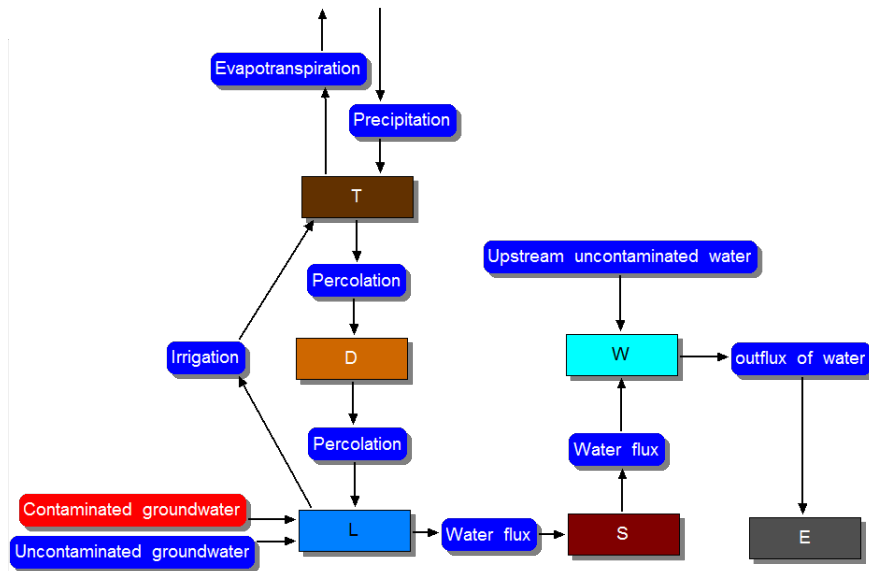


Figure 5: Water fluxes considered in the Reference Case

Solid material fluxes (Figure 6)

Inflow of solid material in the system takes place through surface water and local aquifer as suspended material in the non-contaminated water fluxes (Figure 5). Solid material is moved between compartments by different mechanisms:

- Suspended in water: irrigation, percolation, water flux from L to S and outflow to elsewhere
- Bioturbation: earthworms activity transporting solid material from deep to top soil
- Erosion from the top soil to the river (W)
- Re-suspension of solid material in bed sediments to the surface water

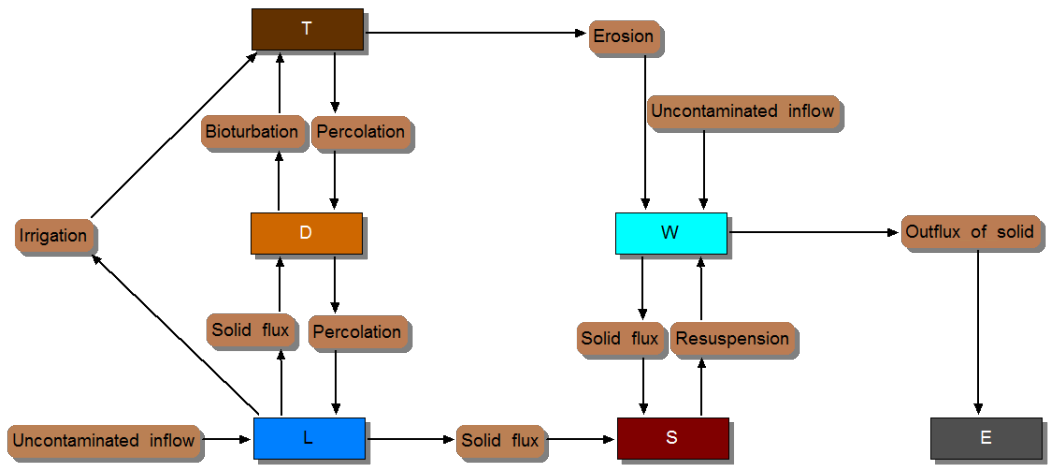


Figure 6: Solid material fluxes considered in the Reference Case

Diffusion

Radionuclide transport by diffusion is considered between adjacent compartments such as top soil – deep soil – local aquifer – bed sediments. Figure 7 shows diffusive transfers between the mentioned compartments.

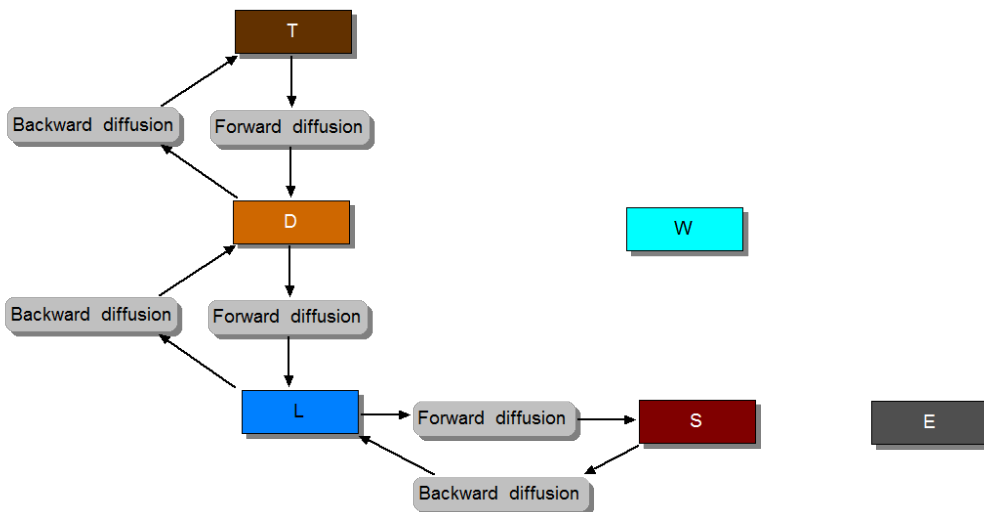


Figure 7: Diffusive fluxes considered in the Reference Case

Radionuclides are transported both dissolved and attached to solid material, according with the fluxes above. Figure 8 shows a summary of all transfer mechanisms considered between all compartments of the biosphere model.

All fluxes will be implemented in AMBER (Figure 4).

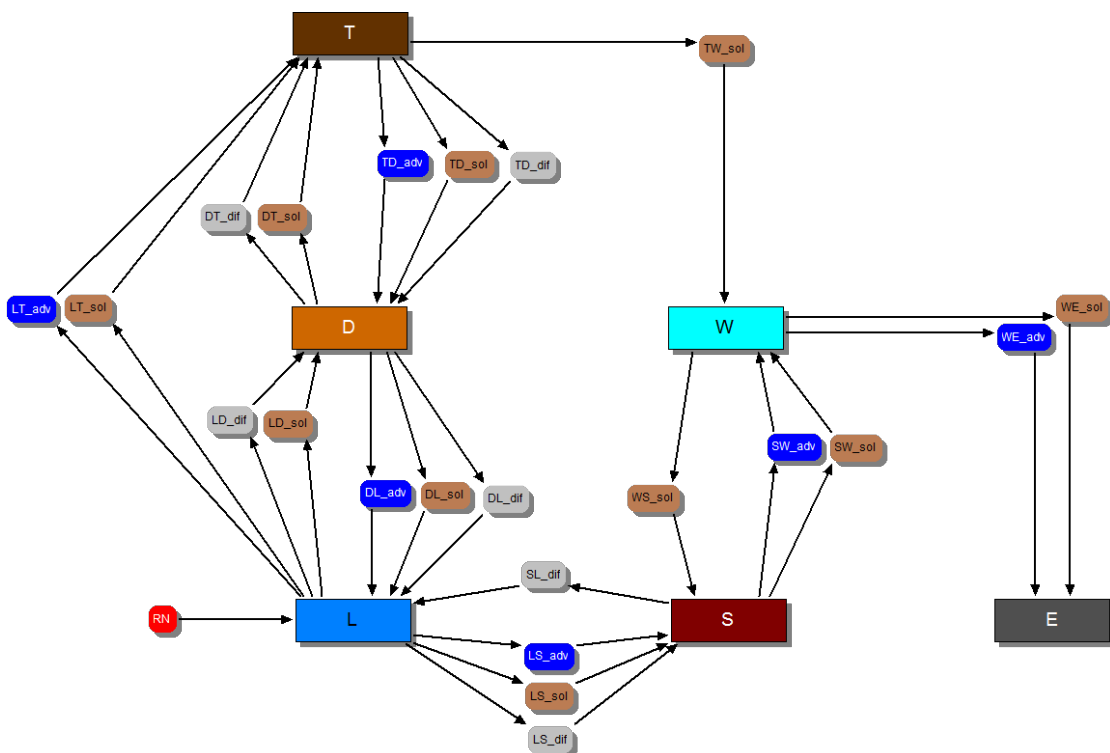


Figure 8: Reference Case model implemented in AMBER © where transferences are split up as function of the radionuclide transport mechanism: advection (blue), diffusion (grey) and sorbed onto solid material (brown)

3.1.2 Exposure pathway sub-model

The exposure pathway sub-model is shown in Figure 9. This part considers all the pathways that an individual of the critical group is exposed to, and that contributes to the annual dose received.

The critical group is representative of the population expected to receive the highest dose. The group represents a community of about 100 inhabitants (small village) and the surface area considered in the study is a region large enough to supply all basic provision for that community from local sources. Individuals are assumed to spend their entire lifetime in the contaminated area. The human diet is derived from present-day Swiss habits.

Dose is calculated as the sum of all pathways (Figure 9), classified as:

- **External** dose: result of the exposition of the individual to external γ -irradiation emitted by the top soil,
- **Inhalation** dose: inhalation of soil particulates present in the atmosphere and
- **Ingestion** dose: ingestion of drinking water and foodstuffs

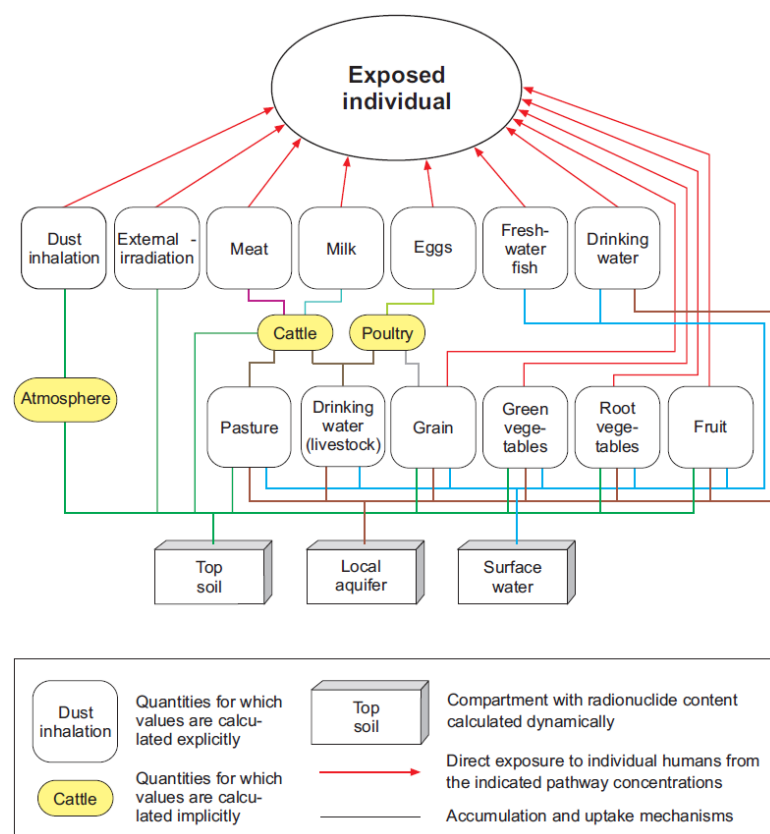


Figure 9: Exposure pathway model showing the relationship between pathways and the physical environment (Nagra 2002a)

The following assumptions have been considered in the exposure pathway model:

- Groundwater abstracted from a well in the local aquifer is used as drinking water and for the irrigation of the agricultural land
- Crops and pasture are grown in a well-mixed rooting zone
- The radionuclides ingestion by livestock occurs via drinking water, fodder and direct consumption of soil
- Fresh-water fish accumulate radionuclides from the river

Dose via each pathway depends on the radionuclide concentration in the physical environment (Table 1). For example, dose via dust inhalation is proportional to the concentration in the top soil compartment, which represents the average over the region of interest.

Table 1: Exposure pathways and their dependence on radionuclide concentration in physical environment compartments

Dose	Exposure pathway	Dependence on RN concentration in...		
		Top soil	Local aquifer	Surface water
External	γ -irradiation	X		
Inhalation	Dust inhalation	X		
Ingestion	Drinking water		X	
	Fresh-water fish			X
	Crop	X	X	
	Green vegetables	X	X	
	Root vegetables	X	X	
	Meat	X	X	
	Milk	X	X	
	Eggs	X	X	

3.2 Numerical model

This section presents the numerical model that describes the conceptual model and allows calculating BDCFs. All expressions used to calculate transfers and doses have been extracted from Klos et al. (1996).

The mathematical representation does not need any special adaptation for its implementation in AMBER© because TAME is also a compartmental modelling code and the way to calculate and develop box models is very similar. It is important to note, before starting the description of the numerical model, the following aspects regarding its implementation in AMBER© (Quintessa Limited 2011):

- Radionuclides are assumed to be uniformly mixed in each compartment
- A compartment is any specific part of the system being modelled (e.g. local aquifer)
- Each transfer is 'donor controlled', depending directly on the radionuclide amount present in the compartment from which RN is leaving.
- It is considered that radionuclides decay into other radionuclides with time

In that case, the system is also split up into two sub-models for their mathematical description.

3.2.1 Physical sub-model

The amount of radionuclide in any compartment with time is determined by Equation 1, taking into account the exchange rates between compartments, the decay of the radionuclide m and its ingrowth due to the disintegration of its parent nuclide $m+1$.

$$\frac{dN_i^m}{dt} = \left(\lambda_i^{m+1} N_i^{m+1} + \sum_j \lambda_{ji} N_j^m + S_i^m(t) \right) - \left(\left[\lambda_i^m + \sum_j \lambda_{ij} \right] N_i^m \right) \quad \text{Equation 1}$$

N_i^m Total amount of radionuclide m in compartment i (Bq)

$S_i^m(t)$ External source term of radionuclide m to compartment i (Bq/y)

λ_{ij} Transfer coefficient between compartment i and compartment j (y^{-1})



λ_i^{m+1}	Decay rate of the parent nuclide $m+1$ (y^{-1})
λ_i^m	Decay rate of the radionuclide m (y^{-1})

The source term (red box in Figure 4) is only considered when calculating the amount in the local aquifer. A normalized constant flux of 1Bq/y of each radionuclide is assumed to enter the system. Decay rates for each radionuclide of interest are presented in the Appendix A: Data used for Reference Case.

Transferences between compartments are characterized by the exchange rate (λ_{ij}) which considers all mechanisms described in the previous section (see 3.1). The general equation used for the calculation of transfer of a contaminant m from compartment i to j integrates advection, diffusion and solid material fluxes (Equation 2).

$$\lambda_{ij}^m = \frac{1}{\theta_i + (1 - \varepsilon_i)\rho_i K_{d,i}^m} \left(\frac{F_{ij} + K_{d,i}^m M_{ij}}{A_i l_i} + D_{ij} \right) \quad \text{Equation 2}$$

λ_{ij}^m	Transfer rate of radionuclide m from compartment i to j (y^{-1})
F_{ij}	Water flux from compartment i to j (m^3/y)
M_{ij}	Solid material flux from compartment i to j (kg/y)
θ_i	Volumetric moisture content of compartment i (-)
ε_i	Porosity of compartment i (-)
ρ_i	Density of the solid material in compartment i (kg/m^3)
$K_{d,i}^m$	Sorption coefficient of radionuclide m in compartment i (m^3/kg)
A_i	Area of compartment i (m^2)
l_i	Thickness of compartment i (m)
D_{ij}	Effective diffusion rate for contaminants in solution moving between compartment i and j (y^{-1})

The calculation of water fluxes, solid material fluxes and effective diffusion rates is shown below.

Water fluxes (F_{ij})

Precipitation, evaporation and irrigation water fluxes (F_{AT} , F_{TA} and F_{LT} , respectively) are calculated converting the specific fluxes (m/y) to volumetric fluxes (m³/y) by multiplying with the surface area of the biosphere (A_f) (Equation 3 to Equation 5).

$$F_{AT} = RAINFALL * A_f \quad \text{Equation 3}$$

$$F_{TA} = ETP * A_f \quad \text{Equation 4}$$

$$F_{LT} = IRRI_L * A_f \quad \text{Equation 5}$$

Inflow fluxes into the biosphere system are provided (F_{UL} , F_{CL} and F_{UW})³ and the rest of water fluxes are obtained by water mass balance (Equation 6 to Equation 10).

$$F_{TD} = (F_{LT} + F_{AT}) - F_{TA} \quad \text{Equation 6}$$

$$F_{DL} = F_{TD} \quad \text{Equation 7}$$

$$F_{LS} = (F_{DL} + F_{UL} + F_{CL}) - F_{LT} \quad \text{Equation 8}$$

$$F_{SW} = F_{LS} \quad \text{Equation 9}$$

$$F_{WE} = F_{SW} + F_{UW} \quad \text{Equation 10}$$

Water flux values, both provided directly by Nagra and calculated as above, are presented in the Appendix A: Data used for Reference Case.

Solid material fluxes (M_{ij})

The calculation of solid material fluxes depends on the transport mechanism of the solids between compartments (see section 3.1). In the following the mechanism and the numerical representation of each transfer considered in the model are summarized (Table 2).

² F_{AT} stands for the precipitation flux from atmosphere (A) to top soil (T), and F_{TA} corresponds to the evapotranspiration (flux from top soil (T) to atmosphere (A))

³ F_{UL} = uncontaminated source flux into local aquifer, F_{CL} = contaminated source flux into local aquifer, F_{UW} = uncontaminated source flux into surface water

Table 2: Numerical terms used for the calculation of solid material fluxes

	Suspended solid material in water flow	Erosion	Bioturbation	Re-suspension
	$\alpha_i F_{ij}$	$M_e A_f$	$W_D M_D A_f$	$\kappa_{SW} V_S (1 - \varepsilon_S) \rho_s$
M_{LT}	X			
M_{UW}	X			
M_{LS}	X			
M_{TW}		X		
M_{LD}		X		
M_{UL}	X	X		
M_{DT}		X	X	
M_{SW}				X

α_i : suspended solid concentration in compartment i (kg/m^3)

M_e : erosion [$\text{kg}/(\text{m}^2\text{y})$]

W_D : activity of earthworms: number of round trips between deep soil and top soil (y^{-1})

M_D : biomass in deep soil material (kg/m^2)

κ_{SW} : turnover rate: bed sediment to suspended solid in water column (y^{-1})

V_S : volume of bed sediment compartment (m^3)

Each of the specified solid fluxes in Table 2 is calculated as the sum of the transport mechanisms considered in each case. For example, solid material flux from deep to top soil (M_{DT}) is obtained applying the formula $M_{DT} = M_e A_f + W_D M_D A_f$.

The erosion term does not only appear in the transfer from top soil to surface water but also in the solid fluxes from local aquifer to deep soil and the subsequent flux to the top soil. The reason is that the thickness of the three compartments is required to be constant to achieve a steady state with the aim to calculate BDCFs. It is a manner to compensate the loss of soil from the top soil.

Mass balance calculations have been implemented for solid material fluxes described in section 3.1 and not cited in Table 2. Equation 11 to Equation 14 show how the fluxes have been obtained.

$$M_{TD} = (M_{LT} + M_{DT}) - M_{TW} \quad \text{Equation 11}$$

$$M_{DL} = (M_{TD} + M_{LD}) - M_{DT} \quad \text{Equation 12}$$

$$M_{WS} = M_{SW} - M_{LS} \quad \text{Equation 13}$$

$$M_{WE} = (M_{UW} + M_{TW} + M_{SW}) - M_{WS} \quad \text{Equation 14}$$

As in the case of water fluxes, all parameters used for solid material fluxes calculations and the final value for each transfer flux are presented in Appendix A: Data used for Reference Case.

Diffusion (D_{ij})

Diffusion is defined by two equations, forward and backward, due to the limitations of the code to introduce non-linear equations. So, diffusion between compartments i and j is represented as in Equation 15 for forward diffusion and the same but with parameters of compartment j for backward diffusion.

$$D_{ij} = \frac{1}{l_i \cdot \min(l_i, l_j)} \frac{D_0 \theta_i}{T_i} \quad \text{Equation 15}$$

D_0 Diffusion coefficient for the radionuclide in solution (m^2/y)

T_i Tortuosity of the medium (-)

3.2.2 Exposure pathway sub-model

Regarding the mathematical representation of the exposure pathway sub-model, Equation 16 gives a general expression for the derivation of the dose received by individuals exposed to radionuclides in the biosphere environment in Sv/y.

$$D_p^m(t) = \sum_{m,exp} E_p H_{exp}^m P_p^m N^m(t) \quad \text{Equation 16}$$

N^m Amount of radionuclide m (Bq)

P_p^m Processing factor: conversion of N^m into a concentration in pathway p

E_p Exposure factor: consumption rate of foodstuff/water or occupancy of the modelled region

H_{exp}^m Dose per unit intake for radionuclide m : conversion of exposure to environmental concentrations of radionuclides into the corresponding dose (Sv/Bq)



Specific expressions for each exposure pathway are presented below. Part of the processing factor that appears in all of them is the concentration of radionuclides in some of the compartments of interest for dose calculation: top soil, local aquifer and surface water (Equation 17). It is the concentration in the compartment taking into account both radionuclide in solution and sorbed in the solid phase.

$$C_T = \frac{N_T}{V_T}, \quad C_L = \frac{N_L}{V_L}, \quad C_W = \frac{N_W}{V_W} \quad \text{Equation 17}$$

When it is important to know the concentration in solution, other parameters such as the porosity or the density of the media should be considered (Equation 18).

$$C_{well}^{drinking\ water} = \frac{1 + (1 - f_{filter})\alpha_L K_{d,L}}{\theta_L + (1 - \varepsilon_L)\rho_L K_{d,L}} C_L \quad \text{Equation 18}$$

f_{filter} Fraction of solid material removed (-)

All formulas used for the calculation of the dose as a result of the exposure to a specific pathway follow the structure of Equation 16. An example is given in the first pathway described below (drinking water).

Drinking-water consumption

Drinking-water is assumed to be all obtained from a well in the local aquifer and not to be filtered before consumption.

Equation 19 shows how the dose received due to the consumption of contaminated water is calculated.

$$D_{well} = H_{ing} I_{wat} f_{well} \frac{1 + (1 - f_{filter})\alpha_L K_{d,L}}{\theta_L + (1 - \varepsilon_L)\rho_L K_{d,L}} C_L \quad \text{Equation 19}$$

H_{ing} Dose per unit intake on ingestion (Sv/Bq)

I_{wat} Total annual intake of drinking-water (m³/y) (see Equation 52)

f_{well} Fraction of drinking-water obtained from a well in the local aquifer (-)



In this case, the amount of radionuclide is implicit in C_L (see Equation 17), the exposure factor is represented by I_{wat} and the processing factor is composed by the rest of the expression (Figure 10). The same correlation occurs for all dose expressions.

$$D_p^m(t) = \sum_{m,exp} E_p H_{exp}^m P_p^m N^m(t)$$

$$D_{\text{well}} = H_{\text{ing}} I_{\text{wat}} f_{\text{well}} \frac{1 + (1 - f_{\text{filter}}) \alpha_L K_{d,L}}{\theta_L + (1 - \varepsilon_L) \rho_L K_{d,L}} C_L$$

Figure 10: Correlation between the general form of dose calculation and the specific expression for dose given by drinking-water consumption

Fish consumption

The annual individual dose due to the ingestion of fresh-water fish is given by Equation 20. The fish concentration factor represents the transfer of a radionuclide from contaminated water through different trophic levels of aquatic foodstuff.

$$D_{ff} = H_{\text{ing}} I_{ff} \frac{K_{ff}}{(1 + \alpha_W K_{d,W})} C_W \quad \text{Equation 20}$$

I_{ff} Intake of fish (kg/y) (see Equation 49)

K_{ff} Fish concentration factor [(Bq/kg)/(Bq/m³)]

Grain consumption

Equation 21 gives the expression to calculate the annual dose received due to the consumption of contaminated grain. Grain could be contaminated in three ways: root uptake, interception of contaminated irrigation water and surface contamination.

$$D_{gr} = H_{ing} I_{gr} \left\{ C_{uptake}^{gr\ root} + C_{irrigation}^{gr\ water-} + C_{contamination}^{gr\ surface} \right\} \quad \text{Equation 21}$$

I_{gr} Annual consumption of grain (kg/y) (see Equation 53)

$C_{uptake}^{gr\ root}$, $C_{irrigation}^{gr\ water-}$, $C_{contamination}^{gr\ surface}$ Radionuclide concentration in grain, each concentration stands for different contamination ways (Bq/kg)

Following, it is presented how to calculate the radionuclide concentration in grain depending on the contamination way.

The concentration in the grain due to root uptake is derived from the concentration of radionuclide in the top soil using the transfer factor from the soil to the plant as it is shown in Equation 22.

$$C_{uptake}^{gr\ root} = K_{gr} \frac{C_T}{\rho_T(1 - \varepsilon_T)} \quad \text{Equation 22}$$

K_{gr} Soil-grain transfer factor [(Bq/kg, grain, fresh weight)/(Bq/kg, soil, dry weight)]

Grain could also be contaminated by intercepting radionuclides from irrigation water coming from a well in the local aquifer (Equation 23).

$$C_{irrigation}^{gr\ water-} = f_{gr} \left(\frac{1 - e^{(-\mu_{gr} Y_{gr})}}{Y_{gr}(W_{gr} + H_{gr})} \right) \left(\frac{F_{LT} \frac{1}{\theta_L + (1 - \varepsilon_L) \rho_L K_{d,L}} C_L}{A_f} \right) \quad \text{Equation 23}$$

f_{gr} Food processing factor for grain (-)

μ_{gr} Irrigation mass-interception factor for grain (m²/kg)

Y_{gr} Yield of grain (kg/m²)

W_{gr} Removal of radionuclides from external surfaces of the crop by weathering (the loss term is implicitly to the soil) (y⁻¹)

H_{gr} Removal of activity by harvesting (removed RN is implicitly transferred to the soil). This is a consequence of the assumption of a closed agricultural system. (y⁻¹)

The food processing factor is a correcting factor that takes into account the removal of contaminants during food preparation, cooking, etc. The interception of contaminated water by crop leaves is mathematically expressed in the first term in brackets. The second one gives the radionuclide concentration in the irrigation water.

Surface contamination is the third way by which grain may be contaminated and it is expressed as Equation 24.

$$C_{\text{contamination}}^{gr \text{ surface}} = f_{gr} S_{gr} \frac{C_T}{\rho_T(1 - \varepsilon_T) + \varepsilon_T \rho_W} \quad \text{Equation 24}$$

S_{gr} Surface contamination factor for grain (m^2/kg)

Green vegetables consumption

Dose given by consumption of green vegetables is calculated in the same way as grain and taking into account the same mechanisms of contamination. However, specific parameters such as surface contamination factor, harvesting rate or transfer factors are different (Appendix A: Data used for Reference Case).

Mathematical formulation regarding green vegetables consumption dose is presented in the following equations (Equation 25 to Equation 28)

$$D_{gv} = H_{ing} I_{gv} \left\{ C_{\text{uptake}}^{gv \text{ root}} + C_{\text{irrigation}}^{gv \text{ water-}} + C_{\text{contamination}}^{gv \text{ surface}} \right\} \quad \text{Equation 25}$$

$$C_{\text{uptake}}^{gv \text{ root}} = K_{gv} \frac{C_T}{\rho_T(1 - \varepsilon_T)} \quad \text{Equation 26}$$

$$C_{\text{irrigation}}^{gv \text{ water-}} = f_{gv} \left(\frac{1 - e^{(-\mu_{gv} Y_{gv})}}{Y_{gv}(W_{gv} + H_{gv})} \right) \left(\frac{F_{LT} \frac{1}{\theta_L + (1 - \varepsilon_L) \rho_L K_{d,L}} C_L}{A_f} \right) \quad \text{Equation 27}$$

$$C_{\text{contamination}}^{gv \text{ surface}} = f_{gv} S_{gv} \frac{C_T}{\rho_T(1 - \varepsilon_T) + \varepsilon_T \rho_W} \quad \text{Equation 28}$$



Root vegetables consumption

Root uptake, interception of water irrigation and surface contamination are also the mechanisms of root vegetables contamination. Dose given by the consumption of root vegetables (Equation 29), as well as their concentration in root vegetables resulting from contamination via root uptake and surface contamination (Equation 30 and Equation 31, respectively) are expressed in the same way as in the case of green vegetables and grain.

$$D_{rv} = H_{ing} I_{gv} \left\{ C_{root\ uptake}^{rv} + C_{water-irrigation}^{rv} + C_{surface\ contamination}^{rv} \right\} \quad \text{Equation 29}$$

$$C_{root\ uptake}^{rv} = K_{rv} \frac{C_T}{\rho_T(1 - \varepsilon_T)} \quad \text{Equation 30}$$

$$C_{surface\ contamination}^{rv} = f_{rv} S_{rv} \frac{C_T}{\rho_T(1 - \varepsilon_T) + \varepsilon_T \rho_W} \quad \text{Equation 31}$$

In the case of the concentration in root vegetables due to the interception of radionuclides from water irrigation, the calculation is slightly different (Equation 32). The reason is that the root is the part of the crop being consumed, therefore the process of translocation must be considered. It refers to the transportation of radionuclides from leaves, where contamination is entering into the plant, to the edible part (roots).

$$C_{water-irrigation}^{rv} = \left(f_{gv} + \frac{T_{rv}}{H_{rv}} \right) \left(\frac{1 - e^{(-\mu_{gv} Y_{gv})}}{Y_{gv}(W_{gv} + H_{gv} + T_{rv})} \right) \left(\frac{F_{LT} \frac{1}{\theta_L + (1 - \varepsilon_L) \rho_L K_{d,L}} C_L}{A_f} \right) \quad \text{Equation 32}$$

T_{rv} Translocation rate (y^{-1})

Fruit consumption

The mathematical representation of the dose received for an individual due to the consumption of fruit is shown in Equation 33. It also considers three ways of fruit contamination and the calculation of the radionuclide concentration in fruit caused by each contamination way is the same as for root vegetables (Equation 34 to Equation 36).

$$D_{fruit} = H_{ing} I_{fruit} \left\{ C_{root\ uptake}^{fruit} + C_{water-irrigation}^{fruit} + C_{surface\ contamination}^{fruit} \right\} \quad \text{Equation 33}$$

$$C_{root\ uptake}^{fruit} = K_{fruit} \frac{C_T}{\rho_T(1 - \varepsilon_T)} \quad \text{Equation 34}$$

$$C_{surface\ contamination}^{fruit} = f_{fruit} S_{fruit} \frac{C_T}{\rho_T(1 - \varepsilon_T) + \varepsilon_T \rho_W} \quad \text{Equation 35}$$

$$C_{water-irrigation}^{fruit} = \left(f_{fruit} + \frac{T_{fruit}}{H_{fruit}} \right) \left(\frac{1 - e^{-\mu_{fruit} Y_{fruit}}}{Y_{fruit} (W_{fruit} + H_{fruit} + T_{fruit})} \right) \left(\frac{F_{LT} \frac{1}{\theta_L + (1 - \varepsilon_L) \rho_L K_{d,L}} C_L}{A_f} \right) \quad \text{Equation 36}$$

Meat consumption

Dose received for meat consumption (Equation 37) considers that meat may have been contaminated via the following ways:

- Livestock drinking-water consumption
 - Livestock consumption of pasture that has been contaminated via interception of irrigation water
 - Livestock consumption of pasture that has been contaminated via root uptake
 - Livestock soil ingestion during grazing
-

$$D_{meat} = H_{ing} I_{meat} K_{meat} \left\{ I_{water}^{livestock} + I_{water-irrigation-pasture}^{livestock} + I_{soil-pasture}^{livestock} + I_{soil}^{livestock} \right\} \quad \text{Equation 37}$$

I_{meat} Annual intake of meat (kg/y) (see Equation 56)

K_{meat} Concentration factor in the animal tissue (day/kg)

$I_{water}^{livestock}, I_{water-irrigation-pasture}^{livestock}, I_{soil-pasture}^{livestock}, I_{soil}^{livestock}$ Daily intake rates (Bq/day)

In the case of dose calculation by meat consumption, radionuclide concentration in meat is given multiplying the daily intakes rates via each contamination way (Bq/day) by the concentration factor in the animal tissue (day/kg).

Daily intake of radionuclides due to drinking water is obtained multiplying their concentration in water obtained from the well by the daily consumption of water by the animal (Equation 38). It is also assumed that all water that livestock drink comes from a well in the local aquifer.

$$I_{water}^{livestock} = I_{wc} \left[f_A \frac{1}{\theta_L + (1 - \varepsilon_L) \rho_L K_{d,L}} C_L \right] \quad \text{Equation 38}$$

I_{wc} Daily water consumption by the animal (m³/day)

f_A Fraction of water obtained from the well (-)

Equation 39 expresses the radionuclide daily intake due to the consumption of pasture contaminated by irrigation. Concentration in pasture is calculated as for crops and then, it is multiplied by the daily consumption of fodder and the ratio of fresh pasture to hay, to obtain the daily intake via this mechanism of contamination.

$$I_{water-irrigation-pasture}^{livestock} = Z I_{pc} \left(\frac{1 - e^{(-\mu_p Y_p)}}{Y_p (W_p + H_{pc})} \right) \left(\frac{F_{LT} \frac{1}{\theta_L + (1 - \varepsilon_L) \rho_L K_{d,L}} C_L}{A_f} \right) \quad \text{Equation 39}$$

Z Ratio by weight of fresh pasture to hay (-)

I_{pc} Daily consumption of dry fodder by the animal (kg/day)

Pasture may also contain radionuclides due to root uptake, and the intake by animals due to their consumption is given as Equation 40 shows.

$$I_{\text{soil-pasture}}^{\text{livestock}} = I_{pc} Z K_p \frac{C_T}{(1 - \varepsilon_T) \rho_T} \quad \text{Equation 40}$$

K_p Soil-pasture transfer factor [(Bq/kg crop, fresh weight)/(Bq/kg soil, dry weight)]

Finally, meat may be contaminated due to the ingestion of soil by the animal. Soil intake occurs during grazing and is expressed in Equation 41.

$$I_{\text{soil}}^{\text{livestock}} = S_{pc} Z I_{pc} \frac{C_T}{(1 - \varepsilon_T) \rho_T + \varepsilon_T \rho_W} \quad \text{Equation 41}$$

S_{pc} Weight fraction of wet soil (-)

Milk consumption

Dose given by milk consumption is expressed as for meat consumption (Equation 42). The reason is that livestock contamination occurs via the same ways which are described in equations from Equation 38 to Equation 41.

$$D_{\text{milk}} = H_{\text{ing}} I_{\text{milk}} \rho_W K_{\text{milk}} \left\{ I_{\text{water}}^{\text{livestock}} + I_{\text{irrigation-pasture}}^{\text{livestock}} + I_{\text{soil-pasture}}^{\text{livestock}} + I_{\text{soil}}^{\text{livestock}} \right\} \quad \text{Equation 42}$$

I_{milk} Annual consumption of milk (m³/y) (see Equation 51)

K_{milk} Distribution factor for milk [Bq/kg)/(Bq/day)]

Regarding milk consumption dose calculation, the only differences with respect to meat calculation are that both the annual consumption and the distribution factor are referred to milk. Furthermore, the milk density is assumed to be equivalent to that of water, to convert volume of milk to mass.

Eggs consumption

The calculation of dose from eggs (Equation 43) is similar to that of meat and milk but considering poultry and the ingestion of grain, instead of livestock and pasture, respectively. Mechanisms by which radionuclides may enter poultry are the same four as in the case of livestock.

$$D_{eggs} = H_{ing} I_{eggs} K_{eggs} \left\{ I_{water}^{poultry} + I_{water-irrigation-grain}^{poultry} + I_{soil-grain}^{poultry} + I_{soil}^{poultry} \right\} \quad \text{Equation 43}$$

I_{eggs} Annual consumption of eggs (eggs/y) (see Equation 48)

K_{eggs} Distribution factor for eggs [Bq/egg]/(Bq/day)

Following, the expressions for the calculation of daily intake of radionuclides for poultry are given (Equation 44 to Equation 47).

$$I_{water}^{poultry} = I_{wp} \left[f_{poultry} \frac{1}{\theta_L + (1 - \varepsilon_L) \rho_L K_{d,L}} C_L \right] \quad \text{Equation 44}$$

I_{wp} Daily water consumption by poultry (m^3/day)

$f_{poultry}$ Fraction of water obtained from the well (-)

$$I_{water-irrigation-grain}^{poultry} = I_{gp} \left(\frac{1 - e^{(-\mu_p Y_p)}}{Y_p (W_p + H_{pc})} \right) \left(\frac{F_{LT} \frac{1}{\theta_L + (1 - \varepsilon_L) \rho_L K_{d,L}} C_L}{A_f} \right) \quad \text{Equation 45}$$

I_{gp} Daily consumption of grain by the poultry

$$I_{soil-grain}^{poultry} = I_{gp} K_{gr} \frac{C_T}{(1 - \varepsilon_T) \rho_T} \quad \text{Equation 46}$$

$$I_{soil}^{poultry} = S_{gr} I_{gp} \frac{C_T}{(1 - \varepsilon_T) \rho_T + \varepsilon_T \rho_W} \quad \text{Equation 47}$$

S_{pc} Fraction of the weight of pasture made up of wet soil (-)

In all mathematical representations of ingestion dose pathways, the annual consumption (I_x) is used. This parameter is calculated considering the annual energy intake from food consumption and the contribution of each type of food. The mathematical way to calculate these consumption rates are presented in the following equations (Equation 48 to Equation 56).

$$I_{eggs} = E_0 \frac{f_{eggs}}{\eta_{eggs}} \quad \text{eggs/y} \quad \text{Equation 48}$$

$$I_{ff} = E_0 \frac{f_{ff}}{\eta_{ff}} \quad \text{kg/y} \quad \text{Equation 49}$$

$$I_{fruit} = E_0 \frac{p_{fruit}}{\eta_{fruit}} \quad \text{kg/y} \quad \text{Equation 50}$$

$$I_{milk} = E_0 \frac{f_{milk}}{\eta_{milk}} \quad \text{m}^3/\text{y} \quad \text{Equation 51}$$

$$I_{wat} = I_{fluid} - I_{milk} \quad \text{m}^3/\text{y} \quad \text{Equation 52}$$

$$I_{gr} = \frac{\eta_{gr} p_{gr}}{p_{veg} E_0 (1 - f_{eggs} - f_{milk} - f_{ff})} \quad \text{kg/y} \quad \text{Equation 53}$$

$$I_{gv} = \frac{\eta_{gv} p_{gv}}{p_{veg} E_0 (1 - f_{eggs} - f_{milk} - f_{ff})} \quad \text{kg/y} \quad \text{Equation 54}$$

$$I_{rv} = \frac{\eta_{rv} p_{rv}}{p_{veg} E_0 (1 - f_{eggs} - f_{milk} - f_{ff})} \quad \text{kg/y} \quad \text{Equation 55}$$

$$I_{meat} = \frac{E_0}{\eta_{meat}} (1 - p_{veg}) (1 - f_{eggs} - f_{milk} - f_{ff}) \quad \text{kg/y} \quad \text{Equation 56}$$

All parameters required to calculate the annual consumption of foodstuff and water for an individual of the critical group are presented in Table 3.

Table 3: List of parameters used in annual intake calculation

Parameter	Units	Description
E_0	kJ/y	Calorific value of food consumed annually
f_i	-	Fraction of annual food energy intake obtained from i
p_{veg}	-	Fraction of annual food energy intake obtained from vegetables, after milk, eggs, fish, and fruits have been taken into account
p_i	-	Fraction of energy intake from vegetable consumption coming from i
η_i	kJ/egg kJ/m ³ or kJ/kg	Food energy content of i

External γ -irradiation

All doses described until now are part of the received dose by ingestion of water and foodstuff. In the exposure pathway model it is also considered external dose by γ -irradiation (Equation 57).

$$D_{ext} = GC_T \quad \text{Equation 57}$$

G Groundshine factor [(Sv/y)/(Bq/m³)]

A semi-infinite plane of uniformly contaminated top soil is assumed. The individual spends one year per year inside the contaminated region. The G value takes into account the γ -ray energy and the self-absorption factors for the soils and human tissue.

Dust inhalation

Radionuclides are inhaled via suspended soil particles whose concentration depends on the sorption coefficient (Equation 58).



$$D_{dust} = H_{inh} I_{air} \left[(O_r a_r + O_f a_f) \frac{C_T}{(1 - \varepsilon_T) \rho_T} \right]$$

Equation 58

H_{inh}	Dose per unit intake on inhalation (Sv/Bq)
I_{air}	Volume of air inhaled annually by the individual (m^3/y)
O_r	Normal occupancy rate (y/y)
a_r	Background dust concentration (normal occupancy situation) (kg/m^3)
O_f	Dusty occupancy rate (y/y)
a_f	Occupational dust concentrations (higher than normal) (kg/m^3)

The term in square bracket stands for the airborne concentration due to dust loading. Two situations may be considered: normal occupational situation (dust background levels) and dusty occupational situation when the dust level is increased due to human activities. In this study it is assumed that an individual spends all year under a normal situation.

4. Comparison exercise

In this section, BDCFs obtained in the frame of the ‘Opalinus Clay’ project from Nagra are compared with the values resulting from this study. Both conceptual model and mathematical representation used in this project are exactly the same as the ones followed by Nagra.

The main difference between calculations is the code used to run the model. The results reported here are calculated by using AMBER©, while Nagra used the TAME code.

Although Nagra gives BDCFs for a list of 25 fission and activation products and 29 radionuclides of the ^{243}Cm (^{235}U), ^{244}Cm (^{232}Th), ^{245}Cm (^{237}Np) and ^{246}Cm (^{238}U) chains (Table 4), the verification of the model has been done for 12 radionuclides (see section 3.1).

Table 4: Radionuclides considered in Nagra exercise. In bold, radionuclides included in this study.

<i>Fission and activation products</i>		<i>Cm chains</i>	
^3H	^{94}Nb	^{244}Cm	^{246}Cm
^{10}Be	^{99}Tc	^{240}Pu	^{242}Pu
^{14}C	^{107}Pd	^{236}U	$^{242\text{m}}\text{Am}$
^{36}Cl	$^{108\text{m}}\text{Ag}$	^{232}U	^{238}Pu
^{41}Ca	$^{121\text{m}}\text{Sn}$	^{232}Th	^{238}U
^{59}Ni	^{126}Sn	^{228}Th	^{234}U
^{60}Co	^{129}I	^{228}Ra	^{230}Th
^{63}Ni	^{135}Cs		^{226}Ra
^{79}Se	^{137}Cs	^{245}Cm	^{210}Pb
^{90}Sr	^{151}Sm	^{241}Pu	^{210}Po
^{93}Mo	^{154}Eu	^{241}Am	
$^{93\text{m}}\text{Nb}$	$^{166\text{m}}\text{Ho}$	^{237}Np	^{243}Cm
^{93}Zr		^{233}U	^{243}Am
		^{229}Th	^{239}Pu
			^{235}U
			^{231}Pa
			^{227}Ac

Biosphere Dose Conversion Factor (BDCF) of a radionuclide m is expressed as the steady-state annual dose given by m and its daughters, when a constant flux of 1Bq/y of m is entering into the system (Equation 59).

$$BDCF_m = \frac{D_T^m}{inflow_m} \quad \text{Equation 59}$$

D_T^m Steady-state annual dose of radionuclide m and its daughters (Sv/y)

$inflow_m$ Constant inflow of radionuclide m in the system (Bq/y)

Figure 11 shows the followed methodology to obtain the BDCFs. A constant flux of 1Bq/y of each radionuclide m is the input of the physical biosphere model. The output is the radionuclide concentration in each compartment of the system. The model is run until steady state is reached and then, doses are calculated.

As presented above (section 3.2), the annual dose is derived from radionuclide concentrations in the top soil, local aquifer or surface water, depending on the exposure pathway. The total annual dose is the result of the sum of doses given by each pathway. This dose is directly the BDCF because it is obtained for an inflow of 1Bq/y (see Equation 59).

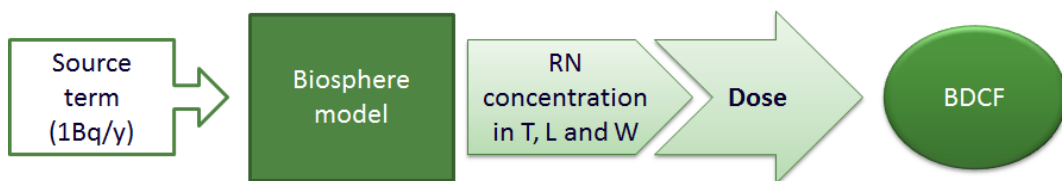


Figure 11: Scheme of the methodology to calculate BDCFs

In the case of the curium chain, the BDCF of each radionuclide includes the contribution of their daughters. For this reason, they are treated separately in the calculations. Two examples are given in Figure 12 a) and b):

- a) ^{246}Cm example: source term is given by an inflow of 1Bq/y of ^{246}Cm . Inflow of their daughters is fixed to zero, so that their concentration will be exclusively due to the decay of ^{246}Cm . The annual dose is calculated for both parent and daughters, giving a BDCF which includes the dose due to 1Bq/y of ^{246}Cm and the dose due to the ingrowth of its decay products.
- b) ^{238}U example: this example shows how radionuclides other than the one studied only contribute to the dose if they are decay products of the parent nuclide (^{238}U in this case). So that in this specific example doses from ^{246}Cm and ^{242}Pu are zero.

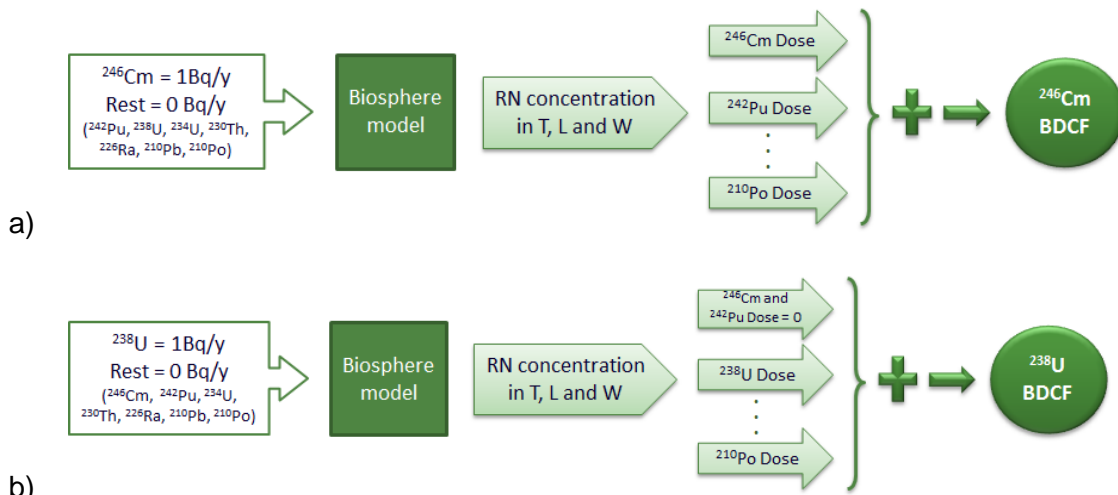


Figure 12: Examples of BDCF calculation when the radionuclide is part of a decay chain. a) ^{246}Cm and b) ^{238}U

The comparison between the BDCF values obtained by Nagra ('Opalinus Clay' project) and by Amphos21 (this project) is presented in Figure 13. The results of this simulation are in agreement with those obtained by Nagra within a $\pm 10\%$ (Figure 14).

These results lead to conclude that the implementation of the model in AMBER© or TAME has not a significant effect over the BDCF calculation. That is because the conceptual model and its mathematical representation are the same and both codes are based on compartmental modelling.

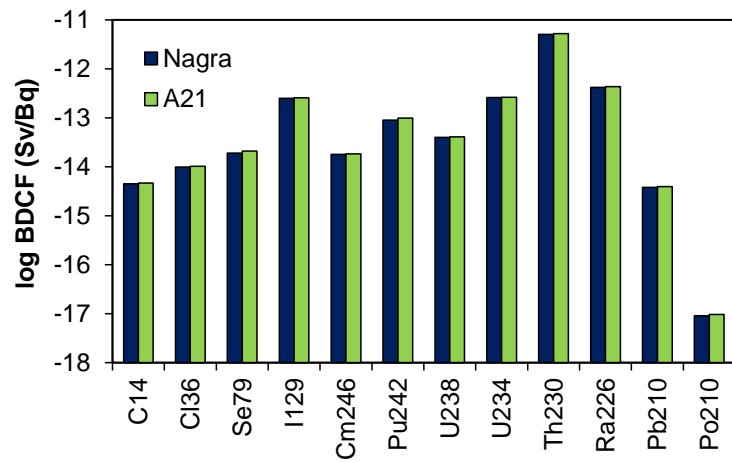


Figure 13: BDCF comparison. Blue columns stand for Nagra results and green columns for the results of this work.

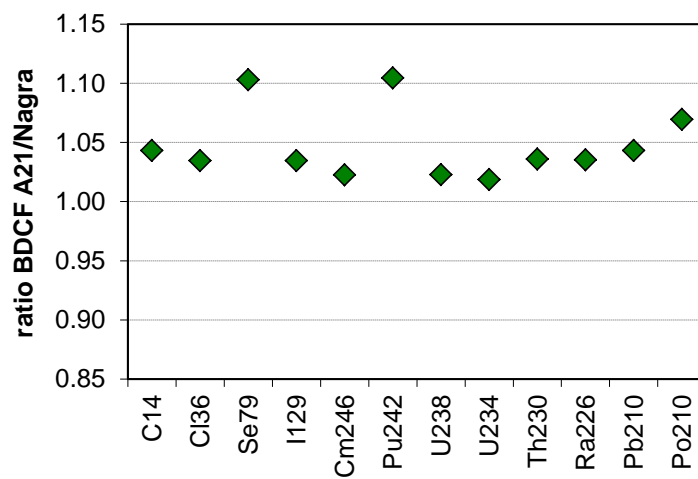


Figure 14: BDCF ratio between this work (A21) and Nagra results

5. Sensitivity analysis

The calculation of BDCF does not only depend on the exposure pathway sub-model but also on the physical biosphere description, as previously presented (Figure 15). Two steps are considered to be relevant for the BDCF assessment. Initially, the physical part is described and modelled defining the compartments of interest and the radionuclide fluxes between them. The output of this step is the radionuclide concentration in each compartment of the system which is the input of the next sub-model (exposure pathway). A detailed dose model is developed considering all the probable pathways that individuals of the critical group may be exposed to. Annual dose is calculated for each pathway and the sum of all of them results on the BDCF value.

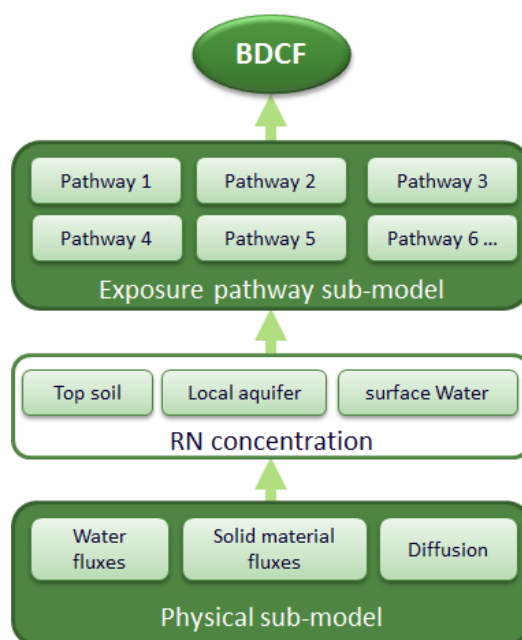


Figure 15: Scheme of the relationships between BDCFs and exposure pathway and physical sub-models.

Considering this relationships between exposure pathways and physical sub-models, any modifications may lead to changes on the value of BDCF. In this section both sub-models are analyzed.

- Exposure pathway sub-model (*Sensitivity test 1*): the contribution of each pathway to the annual dose received by an individual is studied. The aim is to decide whether some of the considered exposure pathways can be neglected in the assessment, and to which radionuclides can the simplification be applied (see section 5.1).
- Physical biosphere system (*Sensitivity test 2*): the radionuclide concentration in the compartments of interest is studied in this case. From the modelling point of view, transferences between compartments are the main processes that can modify RN concentrations. Thus, the test is focused on assessing (see section 5.2):
 - o the impact of solid material fluxes on the concentration of radionuclides responsible for the dose
 - o the influence of diffusion

5.1 Sensitivity test 1 (*Exposure pathway sub-model*)

BDCF values resulting from the Reference Case scenario implemented in AMBER© are presented in Figure 16. From the radionuclides included in this study, ^{230}Th and ^{210}Po are the ones presenting the highest and the lowest BDCF respectively ($5.3 \cdot 10^{-12}$ and $9.7 \cdot 10^{-18}$ Sv/Bq). Other radionuclides with high BDCFs are ^{226}Ra , ^{129}I and ^{234}U ($3.8 \cdot 10^{-13}$, $2.5 \cdot 10^{-13}$, $2.3 \cdot 10^{-13}$ Sv/Bq, respectively).

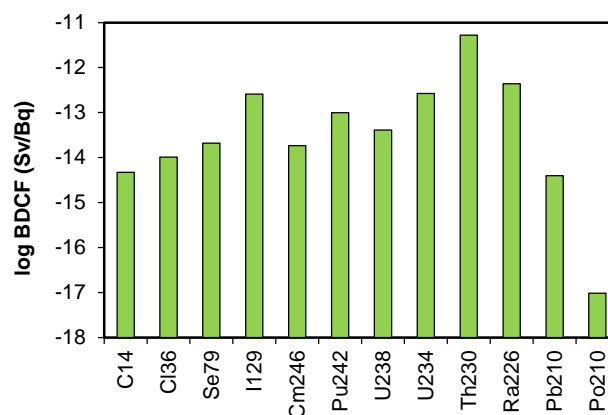


Figure 16: BDCF results from the Reference Case implemented in AMBER©

The contribution of external irradiation, dust inhalation and ingestion of water/foodstuff to the total dose, for each radionuclide, is presented in Figure 17. Ingestion is the main contributor in all cases (>75%) accounting for more than a 99% of the total dose for 9 out of the 12 radionuclides investigated. Dust inhalation has a significant contribution for ^{246}Cm and ^{242}Pu , representing 13 and 23% of the total dose respectively. The contribution to the dose received through external γ -irradiation is below 0.12%.

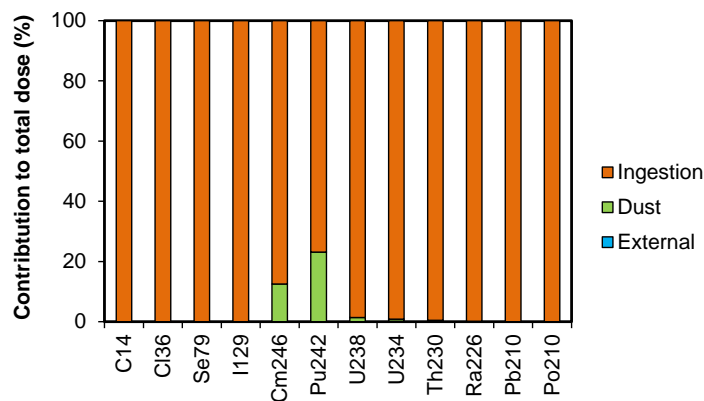


Figure 17: Contribution of external irradiation, dust inhalation and ingestion to total dose

Dust inhalation and external irradiation, respectively, are doses caused by a single pathway, whereas the main contributor to total dose, ingestion, is the result of the sum of several pathways such as consumption of drinking-water, fish, grain, meat, ... Figure 18 indicates the contribution of each pathway considered in the exposure model to the total ingestion dose.

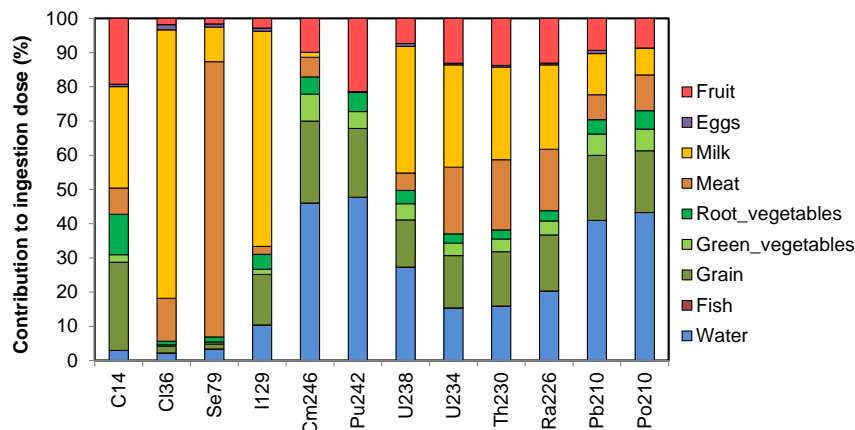


Figure 18: Contribution of ingestion pathways (water and foodstuff) to ingestion dose

The major contributor to the ingestion pathway mainly depends on the type of element. Two distinctive trends are identified, corresponding to non-metallic and metallic (curium chain radionuclides) elements. More than 90% of the dose coming from the ingestion of non-metallic elements is due to the consumption of foodstuff, mainly meat and milk. Ingestion dose from drinking water increases in the case of the curium daughters, responsible for 15 to 50% of the total dose due to ingestion.

Neither fish nor eggs consumption contributes significantly to ingestion dose, accounting for less than a 1.5% of the total ingestion dose.

It is important to highlight that animal and vegetable foodstuff dose considers different contamination ways of the product.

An example is given for the case of milk consumption. Dose is expressed as Equation 42, where four ways of milk contamination are considered. Then, the dose is calculated separately for each contamination way, as presented from Equation 60 to Equation 63.

$$D_{milk} = H_{ing} I_{milk} \rho_W K_{milk} I_{water}^{livestock} \quad \text{Equation 60}$$

$$D_{milk} = H_{ing} I_{milk} \rho_W K_{milk} I_{water-irrigation-pasture}^{livestock} \quad \text{Equation 61}$$

$$D_{milk} = H_{ing} I_{milk} \rho_W K_{milk} I_{soil-pasture}^{livestock} \quad \text{Equation 62}$$

$$D_{milk} = H_{ing} I_{milk} \rho_W K_{milk} I_{soil}^{livestock} \quad \text{Equation 63}$$

The dose given by milk consumption depends on both the radionuclide concentration in the top soil and water extracted from a well in the local aquifer. Therefore, the tendency to sorption is expected to have a major effect on the dose received via milk.

Non-metallic elements tend to have very low sorption coefficients (<0.01 m³/kg), thus, contamination ways considering transfer of radionuclides in the aqueous phase are dominant (blue and green columns in Figure 19). On the contrary, metallic elements

present higher K_d values ($>0.1\text{m}^3/\text{y}$) and soil contamination ways are the major contributors to the milk contamination and to the dose resulting from milk ingestion (orange and yellow columns in Figure 19).

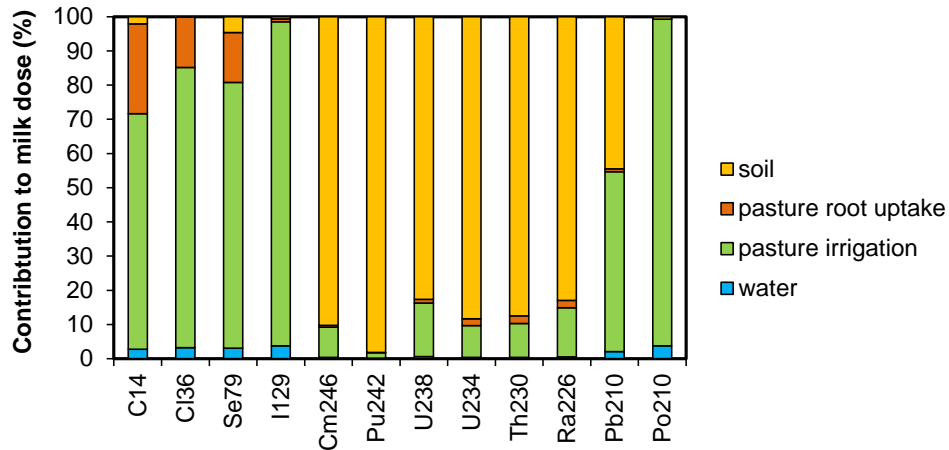


Figure 19: Dose contribution to milk dose depending on the contamination pathway: drinking-water (blue), consumption of pasture contaminated by irrigation water (green) and by root uptake (orange) and consumption of soil (yellow)

To conclude, ingestion is the most important pathway contributor to the dose. Major contributors to the ingestion dose are consumption of drinking-water, meat and milk. The reason for the predominance of a particular ingestion pathway depends on the sorption characteristics of elements. External dose and dose received through fish and eggs consumption can be neglected. It is important to highlight that these conclusions are only valid for the present approach and the radionuclides under study.

5.2 Sensitivity test 2 (*Physical sub-model*)

Radionuclide concentrations in the compartments are needed to adequately calculate the dose received by the individual. RN concentrations mainly depend on the transfer fluxes between different components of the biosphere system. In this section, the effect of radionuclide transport via solid material fluxes and diffusion is studied.

The first step of this analysis is focused on the solid material transfer mechanisms. Five different cases have been considered and compared with the reference case. In each case, one or more solid transfer mechanisms are neglected and, in the last case, all transfer mechanisms of radionuclides sorbed onto solid particulates are eliminated (Table 5).

Table 5: Cases and mechanisms of solid material transport not considered in the model

	Earthworms activity	Erosion	Re-suspension	Suspended material
Reference Case (RC)				
Case 1 (S1)	x			
Case 2 (S2)		x		
Case 3 (S3)	x	x		
Case 4 (S4)			x	x
Case 5 (S5)	x	x	x	x

The impact of the solid material flow modifications on BDCFs is presented in Figure 20. The maximum variability of BDCFs results is obtained for ^{234}U and case 2, where no erosion is considered (2.7 times higher than BDCF of RC). Again, it is observed that sorption properties have an influence on the results. BDCFs of elements with lower K_d (^{14}C , ^{36}Cl , ^{79}Se and ^{129}I), are not affected by solid mass transfer, given their low association with solids. Some changes are on the contrary observed for curium daughters, presenting higher K_d values. The main solid transfer mechanism affecting final values of BDCFs is erosion (green markers in Figure 20) and in some cases activity of earthworms (pink markers in Figure 20) (e.g. ^{226}Ra).

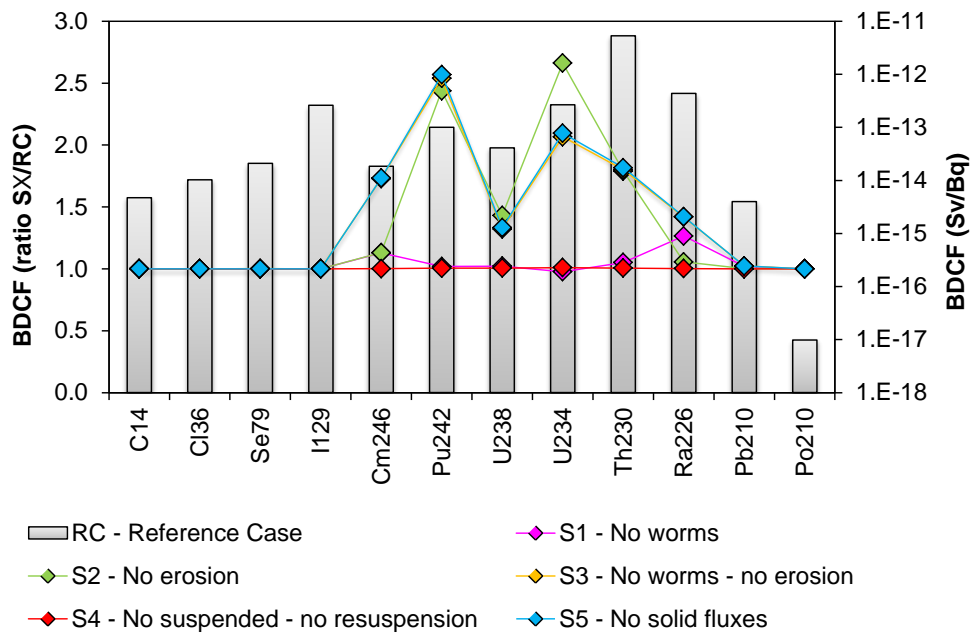


Figure 20: BDCF of each radionuclide in the Reference case (columns, right axis) and the ratio between BDCF obtained in specific case (SX) and reference case (lines with markers, left axis).

It is important to note that, although solid material fluxes are not considered, BDCF are always higher than for the reference case, implying that neglecting solid fluxes is a conservative approach.

The effect observed on BDCFs (Figure 20) is the result of the variation on dose received through each pathway. An example is presented for ^{230}Th , the radionuclide with the highest BDCF in the Reference Case.

The variation noted in the total annual dose to ^{230}Th exposure (directly BDCF, see section 4), is due to the changes produced in the ingestion dose, as shown in Figure 21. Although differences in the dose given by dust inhalation are higher, this pathway does not contribute significantly to the total dose.

The ingestion dose, as well as the total dose, differs from the reference values when erosion is neglected (Figure 22).

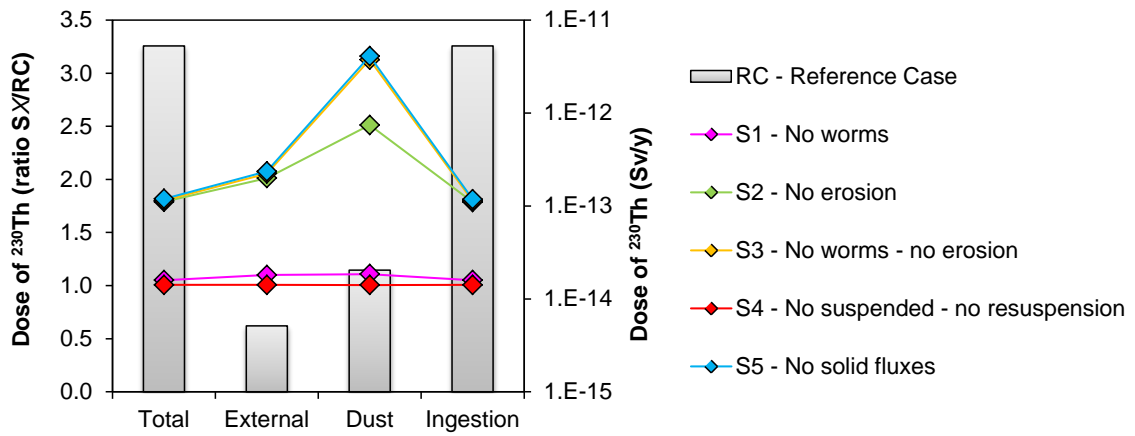


Figure 21: Dose of ^{230}Th as a function of the exposure pathway (columns, right axis) and ratio between dose in SX and RC (lines with markers, left axis)

Neglecting erosion affects all exposure pathways contributing to the ingestion dose. Only meat and milk are slightly affected by earthworm activity, transporting radionuclides sorbed onto solid particulates. Fish consumption is the only pathway whose dose is modified due to the elimination of re-suspension processes.

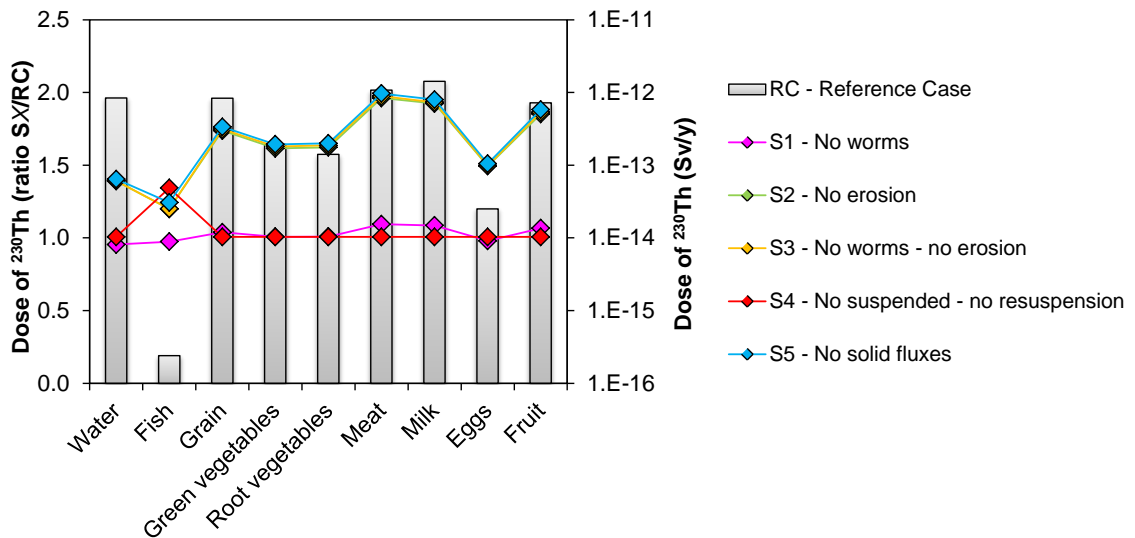


Figure 22: Dose of ^{230}Th as a function of the ingestion exposure pathways (columns, right axis) and ratio between dose in SX and RC (lines with markers, left axis)

The change observed in each exposure pathway is due to the effect that solid fluxes have on the radionuclide concentration in the different compartments. Figure 23 shows how the elimination of the different processes affect the amount of Th in each compartment.

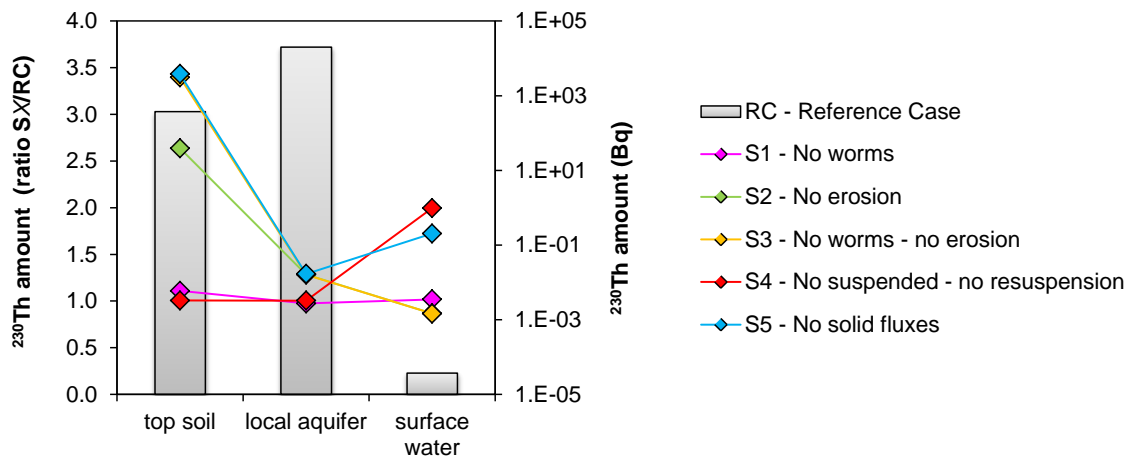


Figure 23: Amount of ^{230}Th in top soil, local aquifer and surface water. In columns is presented the amount in Bq of the reference case (right axis) and in lines with markers, the ratio between the amount in the specified case and the reference case (left axis).

Erosion is the main mechanism affecting the concentration of Th in top soil and local aquifer, while re-suspension is the one producing a higher increase on the concentration in surface water. The effect of not considering solid material fluxes always result in an increase of the thorium concentration which is, at most, 3.4 times that in the reference case (RC).

The increase observed in dose through fish consumption when re-suspension is neglected results from the higher concentration observed in surface water for S4 when compared with the reference case. The same occurs for all pathways although not always directly observed. The reason is twofold:

1. Calculation of doses given by foodstuff depends on the radionuclide concentration of two compartments (local aquifer and top soil) when different mechanism of food contamination are considered

2. ^{230}Th dose values presented do not only consider dose coming from thorium but also that originating from all its daughters. So the observed effect on the final dose is result of the variation on the concentration of all these radionuclides

An example is given in Table 6 where the amount of ^{230}Th in local aquifer and top soil obtained in the reference case (RS) and those obtained when neglecting solid fluxes is presented. Dose resulting from the consumption of milk depending on the contamination mechanism is also shown. In this case, the dose is calculated considering only ^{230}Th and not its daughters. The dose ratio between both cases shows how neglecting solid fluxes results in a dose increase.

Table 6: Amount of ^{230}Th and dose received for consumption of milk contaminated with thorium by different mechanisms in function of RC or S5 case. The ratio between both calculated doses is also presented

	Amount (Bq)		Dose by milk (Sv/y)			
	local aquifer	top soil	Water	Pasture irrigation	Pasture root	Soil
RC - Reference Case	$2.0 \cdot 10^4$	$3.8 \cdot 10^3$	$3.1 \cdot 10^{-18}$	$7.8 \cdot 10^{-17}$	$2.0 \cdot 10^{-17}$	$1.7 \cdot 10^{-15}$
S5 - No solid fluxes	$2.6 \cdot 10^4$	$1.3 \cdot 10^4$	$4.0 \cdot 10^{-18}$	$1.0 \cdot 10^{-16}$	$6.7 \cdot 10^{-17}$	$5.7 \cdot 10^{-15}$
<i>ratio</i>	1.3	3.4	1.3	1.3	3.4	3.4

Consumption of milk contaminated via water ingestion of livestock and the ingestion of pasture irrigated with polluted water leads to a dose 1.3 times higher when neglecting solid fluxes, in agreement with the increase of ^{230}Th in the local aquifer (Equation 38 and Equation 39). In the case where soil is the mechanism of milk contamination either directly by soil consumption or ingestion of pasture contaminated via root uptake, the increase of the dose is in accordance with the increase of the amount of thorium in the top soil compartment.

The same exercise has been done to evaluate the impact of diffusion on BDCFs. Three cases have been compared: S5 (no solid fluxes), S6 where diffusion is not considered and S7 (neither solid fluxes nor diffusion implemented in the model).

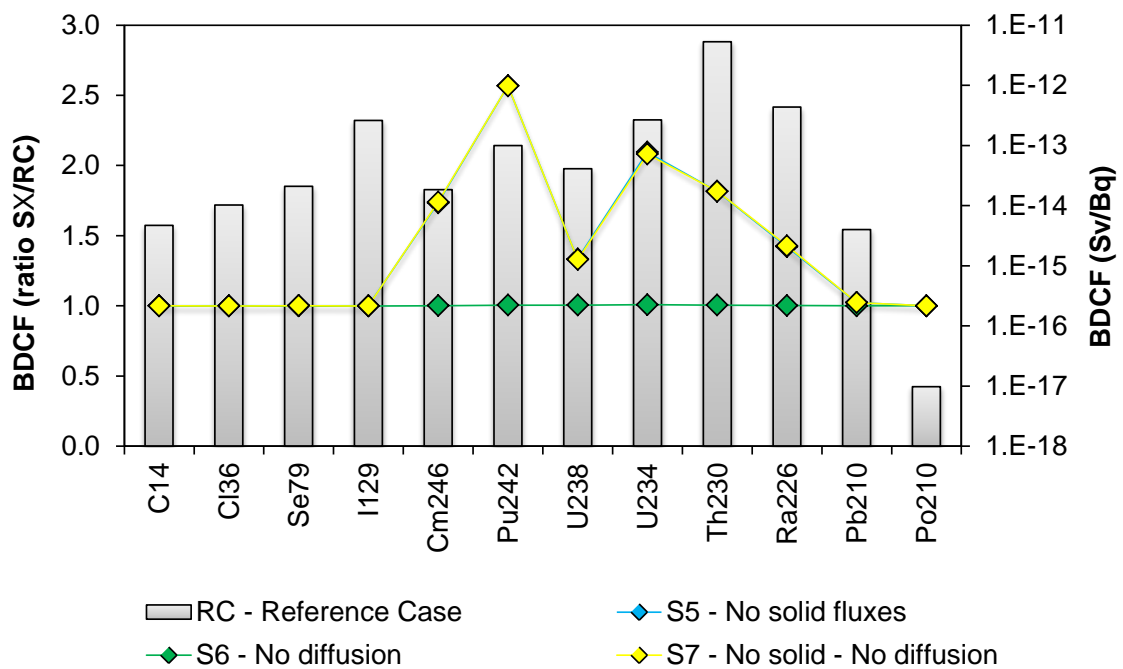


Figure 24: BDCF of each radionuclide in Reference case (columns, right axis) and the ratio between BDCF obtained in specific case (SX) and reference case (lines with markers, left axis).

In the approach considered, transport of radionuclides by diffusion is not an important mechanism and no impact on BDCFs has been observed when omitting diffusion (Figure 24). Results obtained for S7, neglecting solid fluxes and diffusion, are the same as for S5, where only solid fluxes are eliminated. This implies that solid material fluxes are actually affecting BDCF results and that no synergy effects exist when both mechanisms of radionuclide transport are excluded from the simulations.

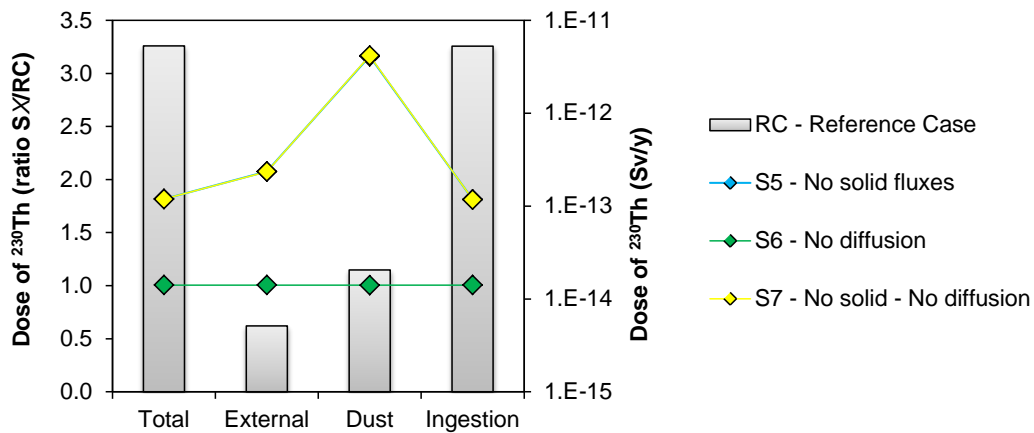


Figure 25: Dose of ^{230}Th as a function of the exposure pathway (columns, right axis) and ratio between dose in SX and RC (lines with markers, left axis)

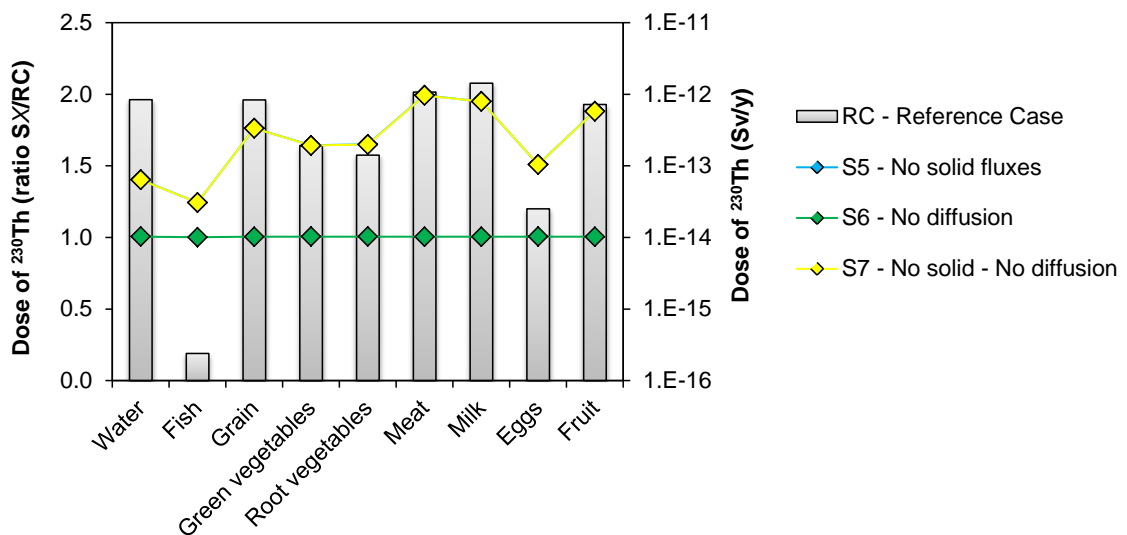


Figure 26: Dose of ^{230}Th as a function of the ingestion exposure pathways (columns, right axis) and ratio between dose in SX and RC (lines with markers, left axis)

Figure 25 and Figure 26 present a comparison of ^{230}Th dose pathways contribution to total and ingestion dose, respectively, as a function of the cases S5, S6 and S7. Same conclusions as for the previous comparison exercise are obtained from both plots:

-
- The increase of total annual dose is the result of increasing of ingestion dose (Figure 25)
 - Meat, milk and fruit consumption are the major contributors to the ingestion dose, and are the ones most affected by the elimination of the solid material fluxes (Figure 26)

Moreover, it can be seen that diffusion has no effect on any exposure pathway considered in that model (Figure 25 and Figure 26). Thus the simplification, for the radionuclides of study here, can be applied.

The reference case takes into account three mechanisms of radionuclide transport: advection, diffusion and solid material transport (Figure 8). From the analysis presented in this section, two different conclusions regarding model simplifications can be drawn:

1. Normal simplification approach (Figure 27): the reference case model may be simplified by disregarding diffusion, re-suspension and suspended particulates in water flux (the latter two as mechanisms of solid material transport). BDCFs resulting from the normal simplification approach do not significantly differ from those derived from the reference case model.
2. Conservative simplification approach (Figure 28): both solid material fluxes and diffusion can be eliminated if conservative calculations are of interest. BDCF results will be slightly higher.

It is important to highlight that all conclusions dealing with simplification tests are only valid for the specific conceptual model used and for the radionuclides selected in this project.

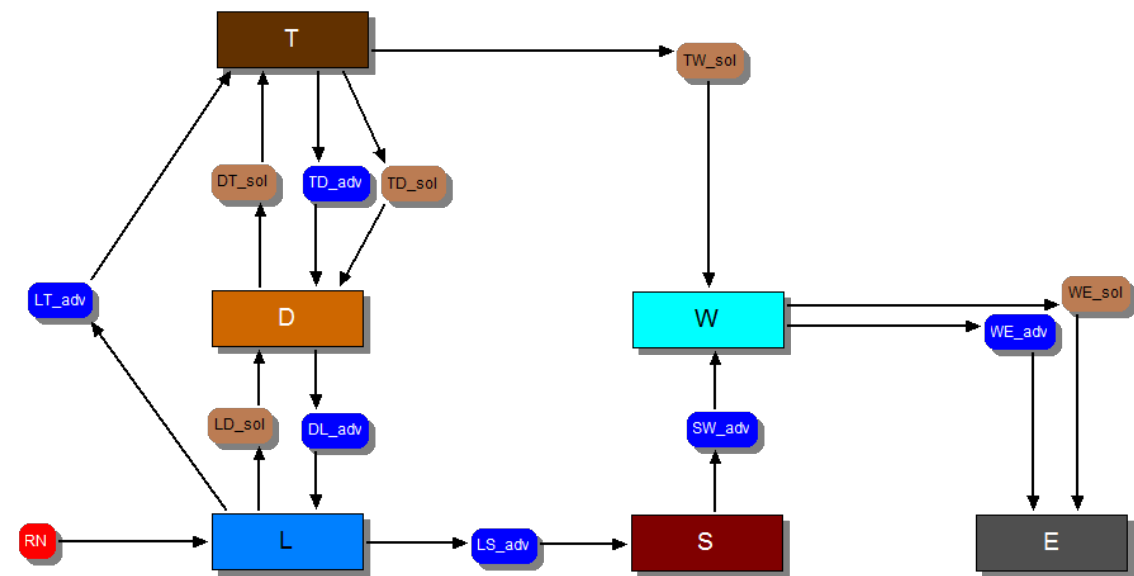


Figure 27: Scheme of simplified model considering normal approach

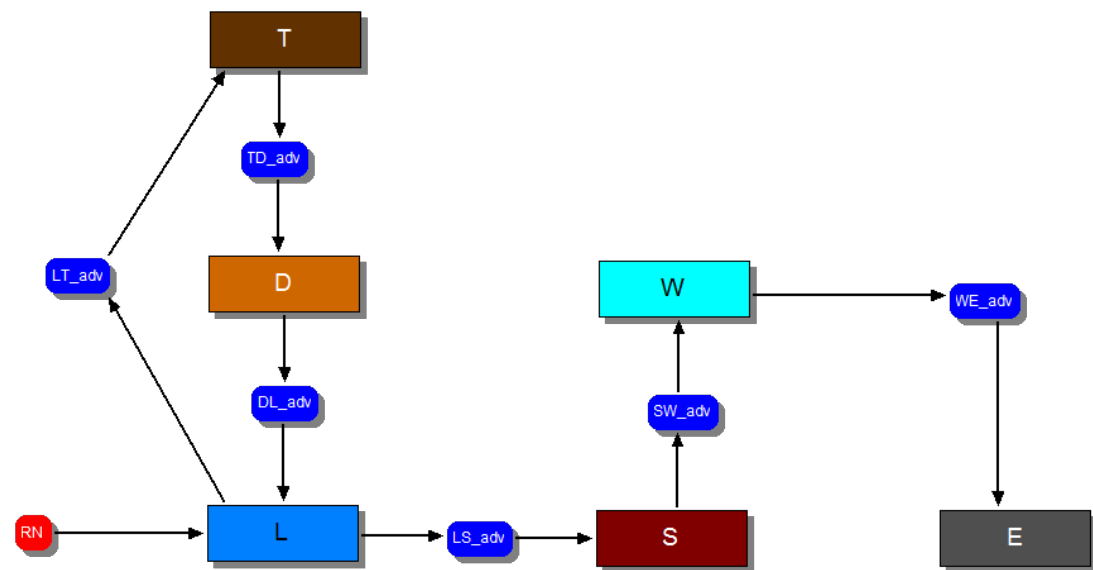


Figure 28: Scheme of simplified model considering conservative approach

6. Contextualization of the Model with other approaches

The aim of this section is to contextualize the Reference Case conceptual model of 'Opalinus Clay' project developed by Nagra with biosphere approaches considered by other organizations in their safety assessment of radioactive waste repositories.

A brief description of the biosphere models developed by different organizations (SKB, Posiva, Andra, NIRONDA and NWMO) and results obtained from the PAMINA project (European project dealing with the Performance Assessment Methodologies in Application to Guide the Development of the Safety Case) is presented below.

6.1 SBK, Sweden

SKB (2011) presents the complete safety assessment for SR-Site which is focused in three fields: performance of the repository, geosphere and biosphere. All information regarding biosphere is compiled in SKB (2010) and it is supported by several reports where more details on different biosphere aspects are given (e.g. conceptual model, scenarios, assumptions, ...).

Dose evaluation in the mentioned assessment is based on Landscape Dose conversion Factors (LDF) which is the annual effective dose of a radionuclide to a representative individual from the most exposed group, resulting from a constant unit release rate of this radionuclide to the biosphere (Avila et al. 2010).

Figure 29 shows a representation of the radionuclide model approach applied for LDF calculations. That model has been implemented in the software package Pandora. Pandora is an extension of codes Matlab and Simulink and it is described in more detail in Ekström (2011).

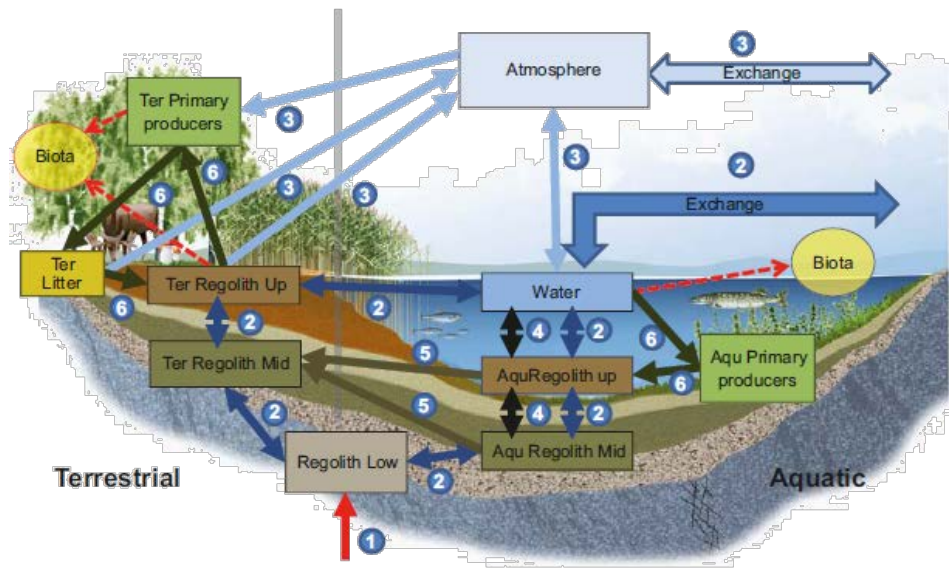


Figure 29: Conceptualization of the Radionuclide model for the biosphere developed by SKB (Avila et al. 2010). Boxes stand for compartments of the system, solid arrows for fluxes and dotted arrows for concentration computations for non-human biota (not included in the mass balance)

The compartment model is composed by 10 biosphere objects (boxes in Figure 29) assumed to be potential receptors of radionuclides released from the repository. Radionuclide transport in the system is related to water, solid material and gas movement. The effect of biota on RN transport between compartments is also considered.

The red arrow in Figure 29 stands for the release of radionuclides from the geosphere entering the biosphere system through the low regolith compartment. After radionuclides reach the biosphere their transport between compartments may occur by different mechanisms (arrows in Figure 29):

- Transport of radionuclides dissolved in water by advection and diffusion (dark blue arrows, 2 in Figure 29)
- Gas emanation and transport (light blue arrows, 3 in Figure 29)
- Radionuclides sorbed onto solid material
 - Sedimentation/re-suspension (black arrows, 4 in Figure 29)

- Terrestrialization (dark brown arrows, 5 in Figure 29)
- Biological uptake/decomposition (green arrows, 6 in Figure 29)

The exposure model uses the activity in different environmental media to calculate doses to human which is an individual representative of the most exposed group. Individuals are assumed to spend all their lifetime in the region of Forsmark and all foodstuff consumed is produced in the contaminated area.

Both external and internal exposures pathways are considered and internal dose comes from inhalation of contaminated air and ingestion of contaminated water and foodstuff.

Four scenarios have been considered, three of them are part of the reference glacial cycle (temperate, periglacial and glacial conditions) and one regarding the global warming climate case.

LDF values obtained for the different scenarios are presented in Figure 30. The assessment has been done for 40 radionuclides although in the figure only the ones of interest for the present study are presented.

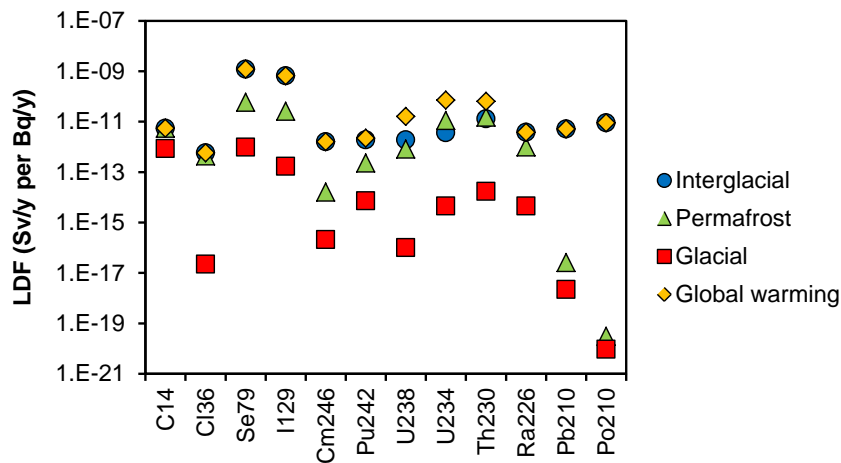


Figure 30: LDF (Sv/y per Bq/y) for the interglacial, permafrost, glacial and global warming scenarios considered by SKB (data from Avila et al. 2010)

Avila et al. (2010) analyse the contribution of the pathways to total annual dose finding that in all cases ingestion of food and water are responsible of more than 90% of the received dose (Figure 31).

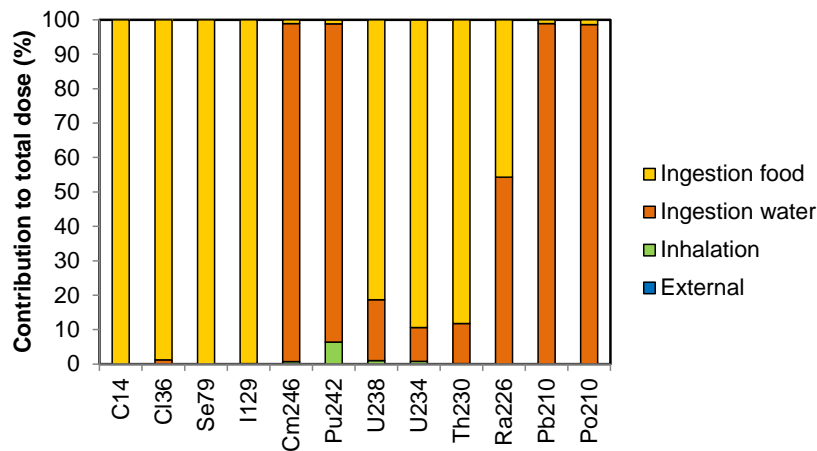


Figure 31: Contribution of external irradiation, dust inhalation and ingestion to total dose of the interglacial scenario (data from Avila et al. 2010)

6.2 Posiva, Finland

Olkiluoto was selected in 2000 as the site for the final disposal repository. Safety analyses are still in progress for the licence application of the disposal facility.

Kyllönen and Keto (2010) carried out a biosphere analysis to obtain dose conversion factors for Olkiluoto. Radionuclide transport models are basically the same as for the ones used for the assessments in the case of the L/ILW waste of the Olkiluoto and Loviisa repositories.

The mentioned study included seven fission products (^{36}Cl , ^{59}Ni , ^{79}Se , ^{93}Mo , ^{94}Nb , ^{126}Sn , ^{129}I and ^{135}Cs) and four scenarios (sea, transition, lake and well scenario). Figure 32 shows a scheme of the lake and well approach where radionuclide flows and dose paths are represented. Sea scenario is not analysed because the dose factors were several orders of magnitude lower than the ones for the transition scenario due to the high dilution in the sea. In addition, the transition model will be simplified because the resulting dose factors were smaller than the ones of the lake and sea scenarios (Kyllönen and Keto 2010).

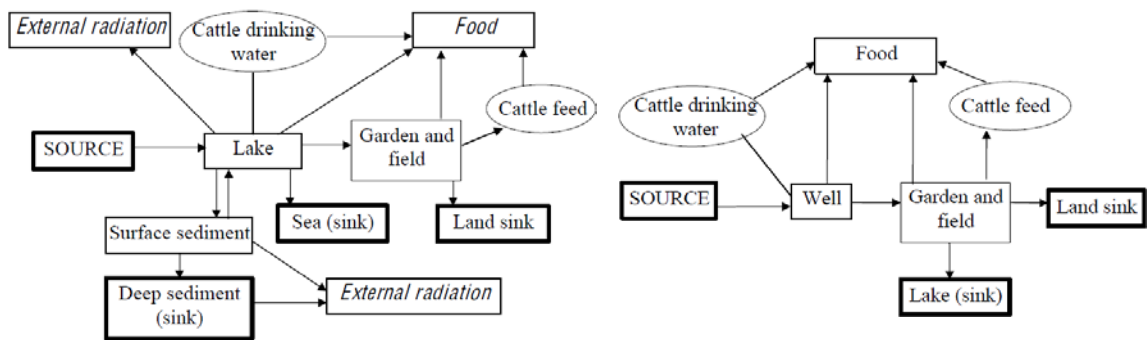


Figure 32: Flow diagrams and dose paths of the lake (left) and well (right) scenario (Kyllönen and Keto 2010)

More details on the mathematical representation and assumptions considered in both scenarios are reported in Kyllönen and Keto (2010). The following figures present the results obtained in the lake and well scenarios (Figure 33 and Figure 34). In both cases, the dose conversion factors (DCF) are represented for the three fission products that are considered in the present project (black markers in figures and right axis). The contribution of the considered exposure pathways to the total dose is also shown. In the lake scenario, consumption of foodstuff (including drinking water) is the only contributor to the ingestion dose.

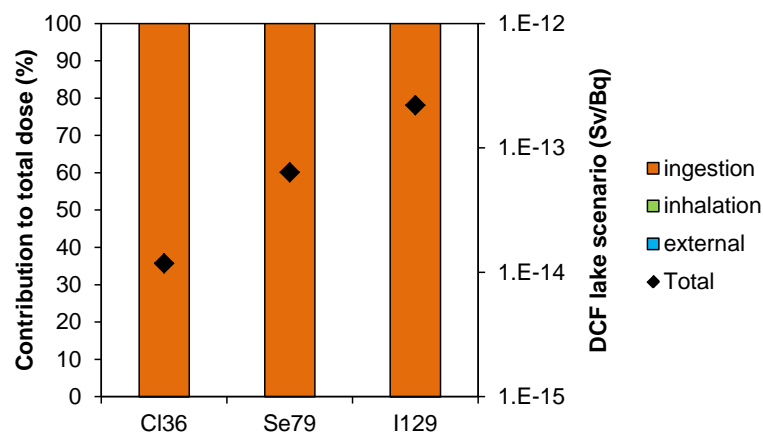


Figure 33: DCF of the lake scenario (markers, right axis) and the relative contribution of ingestion, inhalation and external radiation (columns, left axis) (data from Kyllönen and Keto 2010)

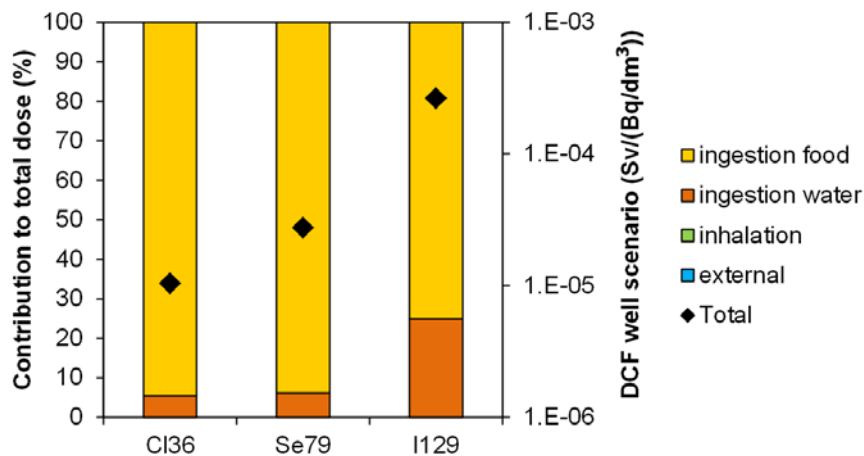


Figure 34: DCF of the well scenario (markers, right axis) and the relative contribution of ingestion of food and water, inhalation and external radiation (columns, left axis) (data from Kyllönen and Keto 2010)

Ingestion is the main dose exposure pathway in the lake and the well scenario. Both dust inhalation and external irradiation are negligible. Their contribution is lower than 0.01%.

The units in which Kyllönen and Keto (2010) report dose conversion factors for the well scenario are different from those of the lake scenario because they are given per rate of abstraction from the well, i.e. normalised to dm^3 , as shown in Figure 34.

Kyllönen and Keto (2010) compare their results with the ones reported in Karlsson and Bergström (2000). In the study of Karlsson and Bergström (2000) the ecosystem specific dose conversion factors (EDF) are obtained by the calculation of the annual dose given by an annual release of 1Bq of each radionuclide. In that case, the list of radionuclides of interest is more comprehensive than in Kyllönen and Keto (2010) including natural chain radionuclides. The conceptual model is based on the approach followed in Sweden for the SR 97 exercise, and the calculation is done for each biosphere object considered (well, lake, running waters, coastal area, agricultural land and peat bog.).

The EDFs obtained from modelling the lake and well scenarios are presented bellow (Figure 35 and Figure 36, respectively). Ingestion is, again, the main exposure pathway but, in the case of some radionuclides of the curium decay chain (^{246}Cm , ^{242}Pu and ^{230}Th) dust inhalation represents almost 50% of the total dose.

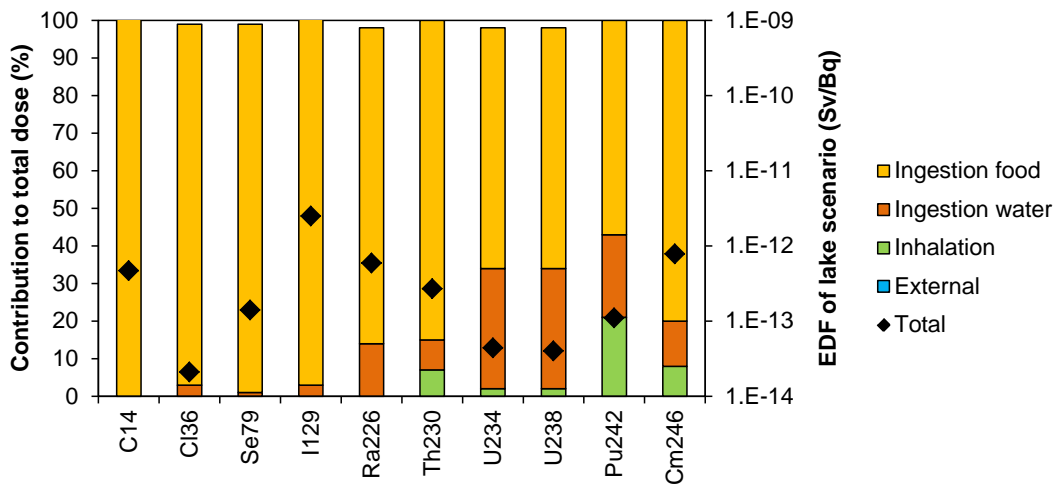


Figure 35: EDF of the lake scenario (markers, right axis) and the relative contribution of ingestion of food and water, inhalation and external radiation (columns, left axis) (data from Karlsson and Bergström 2000)

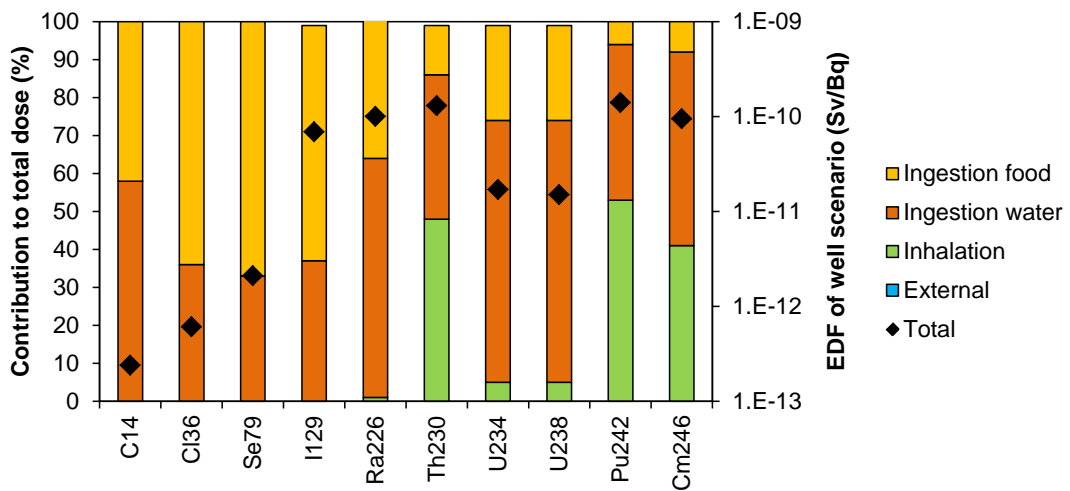


Figure 36: EDF of the well scenario (markers, right axis) and the relative contribution of ingestion of food and water, inhalation and external radiation (columns, left axis) (data from Karlsson and Bergström 2000)

6.3 Andra, France

A description of the biosphere modelling and the calculation of dose conversion factors are reported in Albrecht et al. (2005). Three reference biospheres have been identified as the ones that may potentially occur in the region of Meuse/Haute-Marne which are temperate biosphere, boreal biosphere and tundra biosphere (from the former to the latter, both temperature and precipitation decrease).

The biosphere model is developed assuming that radionuclides reach the system through water compartments. From there, radionuclides are transferred to the rest of the physical components of the system (atmosphere, soil), non-human and human biota. The transfer model is represented as a compartment model shown in Figure 37.

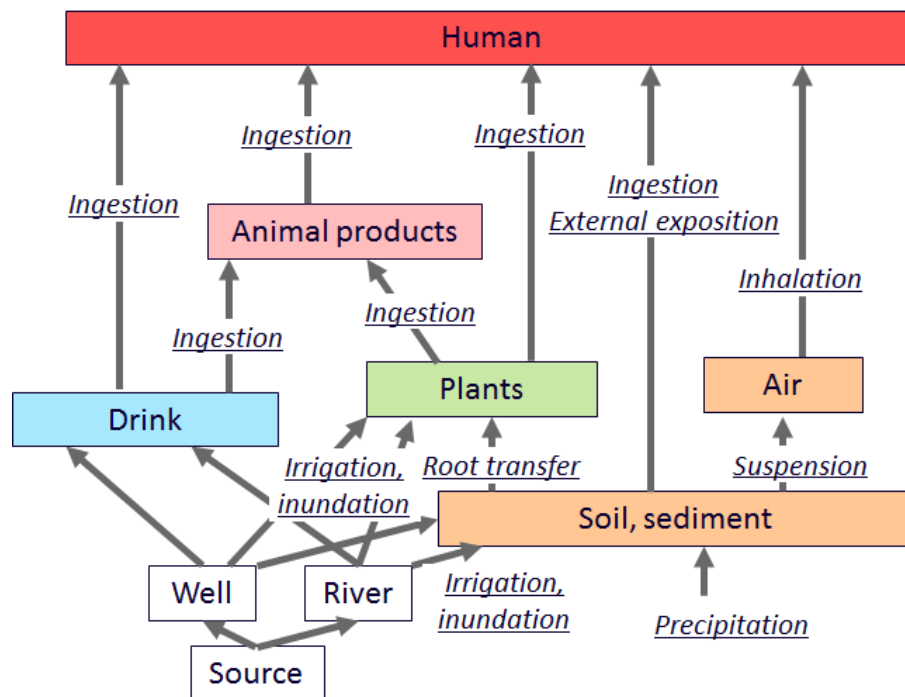


Figure 37: Compartmental model and exposure pathways to human dose (translated from Albrecht et al. 2005)

Dose conversion factors are obtained separately when considering the release from the geosphere to the well or the river. The analysis has been done for 59 radionuclides. The results obtained for the well scenario in the temperate reference biosphere for the

nuclides studied in the present report are shown in Figure 38. Generally, radionuclides of the curium decay chain are the ones with a higher dose conversion factor. Albrecht et al. (2005) found that the dose received for individuals exposed to these radionuclides comes mainly from the ingestion of water and foodstuff. However, some exceptions are observed for specific radionuclides such as ^{59}Nb (not treated in the present study) whose dose is mostly given by external irradiation.

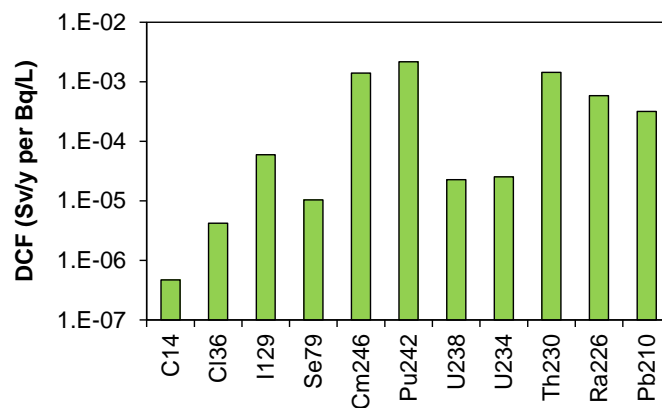


Figure 38: Dose conversion factor (DCF) in Sv/y per Bq/L for the well scenario in the temperate reference biosphere (data from Albrecht et al. 2005)

Probabilistic calculations have been performed by Albrecht and Miquel (2010) for two radionuclides (^{135}Cs and ^{79}Se). Three exercises have been carried out:

1. Introduction of the probabilistic values of all selected parameters.
2. Introduction of only the probability functions of the parameters related with the physical system (e.g. precipitation or distribution coefficients).
3. Introduction of probabilistic valued for societal parameters (food consumption or spent time in contaminated area).

The mean conversion factor for ^{79}Se obtained from the first exercise ($5.8 \cdot 10^{-6}$ Sv/y per Bq/L) was lower than the value of the deterministic calculations from the Albrecht et al. (2005) study ($1.0 \cdot 10^{-5}$ Sv/y per Bq/L). However, the latter is in the range of two standard deviations ($2.0 \cdot 10^{-5}$ Sv/y per Bq/L). Analysing results from all exercises, the authors conclude that the overall uncertainty of dose conversion factors is mainly due to the uncertainties of physical parameters.

6.4 NIROND, Belgium

Biosphere modelling is part of the safety assessment carried out since the 1980s in the Belgian approach. The last published report is SAFIR 2 (Safety Assessment and Feasibility Interim Report) (NIROND 2001) where the work performed from 1990 to 2000 is reported. SAFIR reports have the objective to advice on the qualities of the Boom Clay Formation located at the Mol-Dessel site which is the potential area for the construction of the final and irreversible disposal of Belgian high level wastes.

Dose conversion factors (DCF) are calculated as the maximum annual dose per unit of input flux or per unit of concentration of the radionuclide in the biosphere receptor concerned. Biosphere receptors are the medium in the biosphere that will receive the radionuclides after their migration through the aquifer (NIROND 2001). In that assessment, the following receptors have been considered:

- Well
- Surface water
 - Small water courses: Witte Nete and Desselse Nete
 - Larger water courses, rivers: Kleine Nete (two sections considered: up and downstream)
- Soil

In all cases, radionuclides are assumed to reach the biosphere system through the aquifer and afterwards, they are transported to the rest of the biosphere receptors. In each receptor the DCF is calculated.

The exposure pathway model differs in function of the biosphere receptor in which DCF is calculated. A summary of the exposure pathways considered in each biosphere receptor is presented in Table 7.

Table 7: Types of exposure of the critical group for each biosphere receptor (X = exposure pathway considered, O = exposure pathway not considered)

Type of exposure	Cause of contamination	Well	Desselse Nete	Witte Nete	Kleine Nete	Soil
Ingestion of						
Drinking water		X	O	X	X	O
Food crops	Irrigation	X	X	X	X	O
Food crops	Soil	O	O	O	O	X
Meat/milk	Irrigation	X	X	X	X	O
Meat/milk	Watering of cattle	X	X	X	X	O
Meat/milk	Soil	O	O	O	O	X
Fish		O	O	X	X	O
Inhalation of re-suspension						
On fields/pasture	Irrigation	X	X	X	X	O
On fields/pasture	Soil	O	O	O	O	X
Inhalation of radon exhalation						
On fields/pasture	Irrigation	X	X	X	X	O
On fields/pasture	Soil	O	O	O	O	X
External irradiation						
On fields/pasture	Irrigation	X	X	X	X	O
On fields/pasture	Soil	O	O	O	O	X
On banks of water courses		O	O	X	X	O

Figure 39 shows the results obtained for each biosphere receptor. The highest DCF in all cases are given by ^{79}Se , ^{230}Th and ^{226}Ra . Besides the scenarios listed before, an additional one, neglecting agriculture, is considered. This scenario has been also calculated because water balance of the considered soil does not normally allow for agriculture under present day condition. Thus, including agriculture results in a conservative approach.

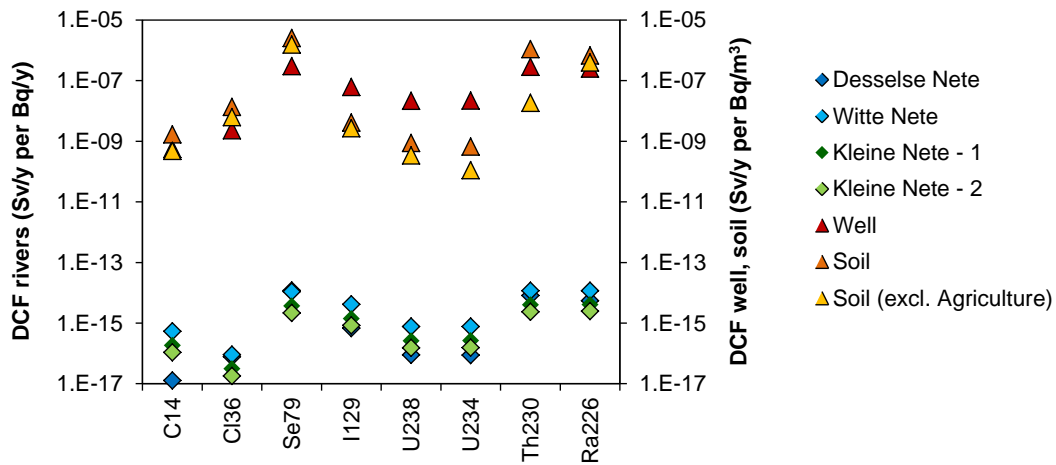


Figure 39: Biosphere dose conversion factors (DCF) per receptor: rivers (Sv/y per Bq/y) (rhombus, left axis) and well and soil (Sv/y per Bq/m³) (triangles, right axis) (data from NIROND 2001)

6.5 NWMO, Canada

The Nuclear Waste Management Organization (NWMO) is responsible of the long-term management of Canada's used nuclear fuel. They develop the Canadian Concept-Generation 4 (CC\$4) system model for postclosure safety assessment of a deep geologic repository for spent CANDU fuel. The model consists of five interlinked sub-models: the wasteform, the containers, the engineered barriers, the geosphere and the biosphere.

The mentioned project has been focused on the description of the biosphere sub-model. The biosphere system has been divided into four sub-systems for calculation purposes:

- a) Surface water
- b) Soil for a garden and forage field
- c) Local atmosphere
- d) Food chain

Radionuclides escaping the geosphere may come into the biosphere system via three ways: the well, the lakebed sediments and the soils at the top of the saturated aquifer.

Dose calculations are performed for an individual of the most exposed group living near the discharge areas. Individuals of the critical group are supposed to spend all their lifetime in the contaminated area and to be self-sufficient (no import of food from outside the region of study).

In the following the four sub-models of the biosphere system are briefly described.

- a) Surface water sub-model (Figure 40): it is assumed that all radionuclides discharged from the geosphere arrive to the lake. Several processes such as runoff, atmospheric suspension, deposition and sedimentation are considered.

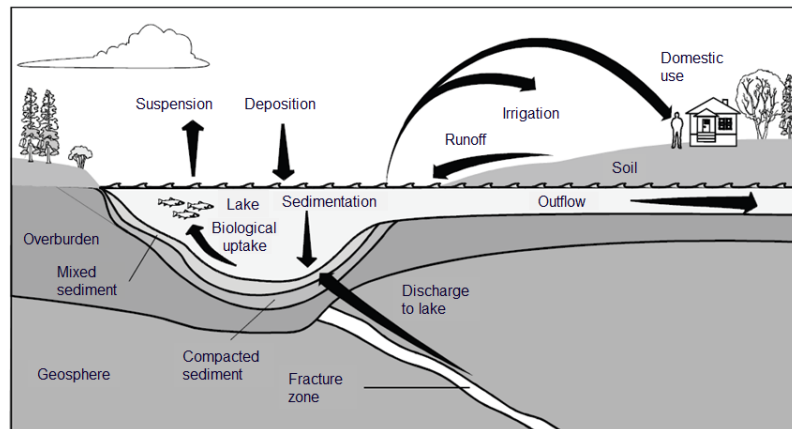


Figure 40: Transport processes considered in the lake (surface water) sub-model (NWMO, 2011)

- b) Soil sub-model for a garden and forage field (Figure 41): this model calculates the concentration of contaminants in the surface (rooting or cultivated) soil layer. Radionuclides can be transferred to the soil by irrigation with water extracted from a well or the lake.

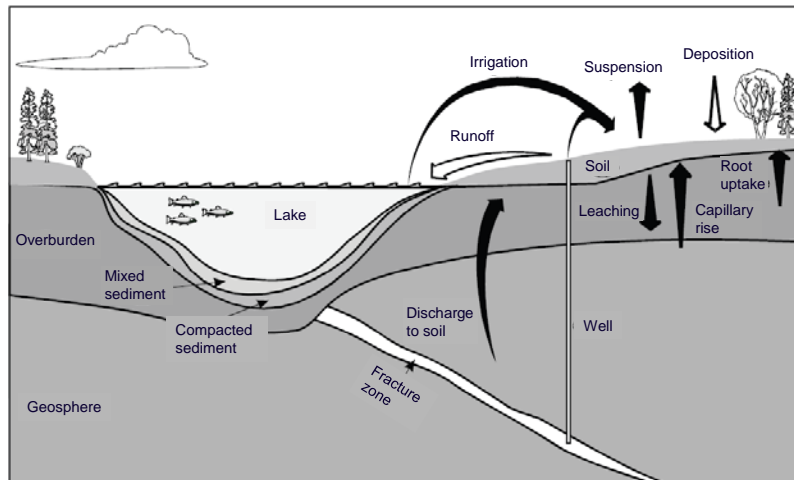


Figure 41: Transport processes considered in the soil sub-model (NWMO, 2011)

- c) Atmosphere sub-model (Figure 42): this model tries to calculate radionuclide concentrations in air resulting from the suspension of particulates and gases from soils, vegetation and water bodies.

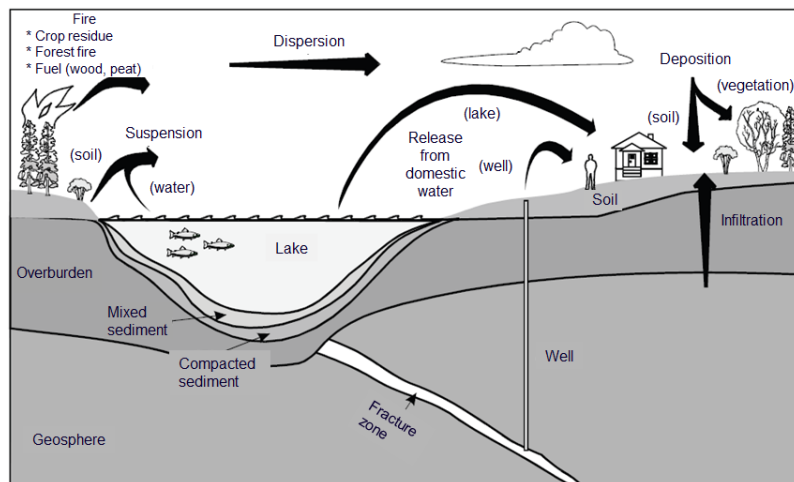


Figure 42: Transport processes considered in the atmosphere sub-model (NWMO, 2011)

- d) Food chain (Figure 43): the aim of this sub-model is to calculate the dose to humans from all important exposure pathways. That calculation depends on the radionuclide concentration in the biosphere compartments which has been

obtained from the previous three sub-models. Different ways of animal and plant contamination have been considered: root uptake, leaves, inhalation and water/soil/plants ingestion.

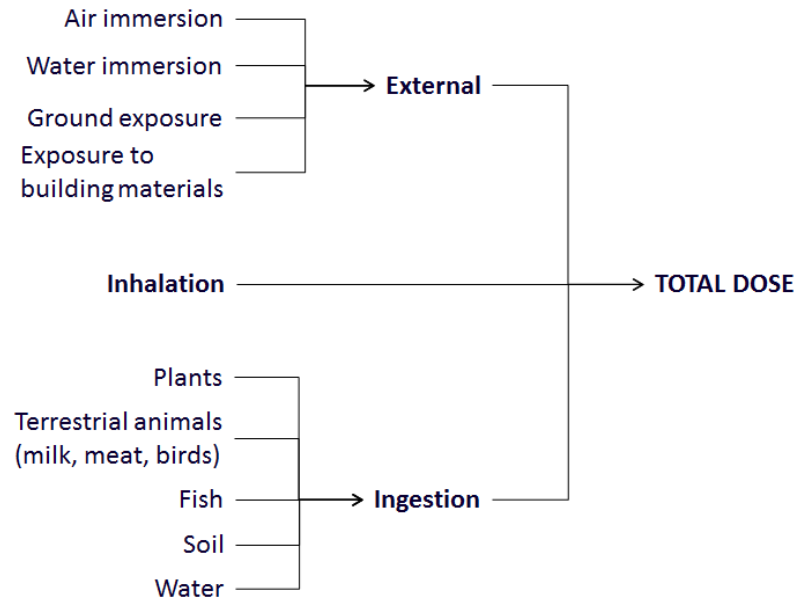


Figure 43: Scheme of the exposure pathways considered in the food chain and dose model.

6.6 PAMINA, European project

PAMINA was an integrated project part of the 6th framework programme of the European Commission called *Performance Assessment Methodologies in Application to Guide the Development of the Safety Case*. The aim of the project was to improve and harmonise methodologies and tools for demonstrating the safety of deep geological disposal of long-lived radioactive waste and spent fuel in different geological environments. The project finished in 2009 and all published information are available at <http://www.ip-pamina.eu/>.

A comparison of the methodologies and tools used by different countries for developing biosphere models was presented in Galson et al. (2009).

A list of participants and the tools and databases they used for the biosphere modelling and dose assessment is presented in Table 8.

Table 8: Summary of tools and databases used in biosphere and dose assessments by the participants (Galson et al. 2009)

Participant	Country	Tool / Database	Purpose
FANC	Belgium		No information supplied
ONDRAF/NIRAS & SCK/CEN	Belgium		No information supplied
NRI & RAWRA	Czech Republic	Excel, AMBER, GoldSim v9.6, RESRAD v6.4	Algebraic expressions and data are encoded in Excel. For some applications the other codes are employed and results are used for Quality Assurance (QA).
POSIVA	Finland	GIS database, UNTAMO toolbox	Details of the landscape elevations and other spatially bounded data. UNTAMO handles the site data using the ArcGIS environment. Interfaced to the biosphere
		POTTI database	Research database for site descriptive data.
		BSAdb	Biosphere assessment database - used for assessment data (in conjunction with other external databases).
		PANDORA / EIKOS	Technical implementation of the biosphere models based on Matlab/Simulink. PANDORA is developed in conjunction with SKB, Sweden, EIKOS is used for sensitivity analysis.
Andra	France	EMOS, EXCON, EXMAS	EMOS is an integrated package for safety assessment including the modules EXCON and EXMAS for calculation of the radiation exposure from radionuclide concentrations or fluxes.
GRS-B	Germany	EMOS, EXCON, EXMAS	EMOS is an integrated package for safety assessment including the modules EXCON and EXMAS for calculation of the radiation exposure from radionuclide concentrations or fluxes.
GRS-K	Germany		No information supplied



		FEP database	Library of FEPs for the assessment model.
NRG	Netherlands	MiniBIOS	Distributions of the DCFs for radionuclides transported via groundwater.
		EXPOS	Radiation EXPOSure in terms of maximum dose rates for individuals.
		UNSAM	Code developed to conduct sensitivity and uncertainty analyses of mathematical models.
ENRESA	Spain	AMBER	Modelling tool in which the assessment model is implemented. Used for both deterministic and probabilistic calculations.
NDA	UK		No information supplied

The authors analysed the approaches of all participants identifying similarities and discrepancies between them. Commonalities and differences between the biosphere description and treatment are summarised below.

- *Phased approach to assessment:* the complexity of the biosphere model evolves with the progress of the disposal programme.
- *The exposure mechanism considered:* exposure pathways considered are similar between agencies: consumption of foodstuff and water, inhalation of dust and external irradiation. Dose coefficients for ingestion and inhalations are selected from ICRP in all cases but conversion factors that give external γ -dose are not the same.
- *Assumption of present-day conditions and consideration of climate-change scenarios:* Present day conditions used as benchmark for future radiological impacts. Different climatic scenarios are also defined. Some agencies take into account human activities.
- *Dose constrains and timescale/situation dependency:* Euratom Directive 96/29 provides a dose constraint value of 1mSv/y for member of the public but regulators in different countries may have adopted more strict limits, generally, 0.1, 0.25 or 0.3 mSv/y. Regarding timescale issue, most of the participants

conduct 10,000 years of quantitative dose evaluations. In addition, results should be interpreted as illustrative measures to complement other safety indicators due to the high uncertainty of evaluating such a long period of time.

- *Regulatory guidance/ fixed parameters, exposed groups:* the evaluation is referred to a critical group that is generally defined by present day habits and practices. Sometimes more than one exposed group is identified, each showing differences in location and lifestyle.
- *Food consumption rates:* in general an average of present-day food consumption rates is used; it is assumed that all food comes from the most contaminated area. Consumption rates for future climate scenarios are based on present-day analogous sites. .
- *Age groups considered:* Usually a unique age group of adults; some agencies define different age groups.
- *Assessment philosophy:* pessimistic, cautious, or equitable.
- *Deterministic vs. probabilistic modelling:* Most of the participants performed deterministic evaluations but in some countries probabilistic calculations have been conducted.
- *Use of radionuclide-specific biosphere models:* generic models are implemented for most radionuclides. Some exceptions are made for ^3H , ^{14}C , ^{36}Cl , ^{79}Se and ^{129}I .
- *Non-human biota:* generally it is not considered due to difficulty in conceptualization and parameterisation
- *Health effects:* only radiological effects are considered and only some organizations include chemical toxicity of radionuclides.

6.7 BDCF comparison

In this section, BDCF obtained in this work by following the ‘Opalinus Clay’ project approach developed by Nagra (grey columns in Figure 44) are compared with the results from the biosphere models from other radioactive waste management agencies (markers in Figure 44) described in previous sections (from section 6.1 to 6.4).

In the graph (Figure 44), dose conversion factors calculated from a unity influx source (1Bq/y) and not the ones from a unit concentration source (1Bq/L) are plotted.

A wide range of DCF values is observed for all radionuclides selected in this project. The maximum difference (6 orders of magnitude) is obtained for ^{210}Po between SKB and the Nagra approach results.

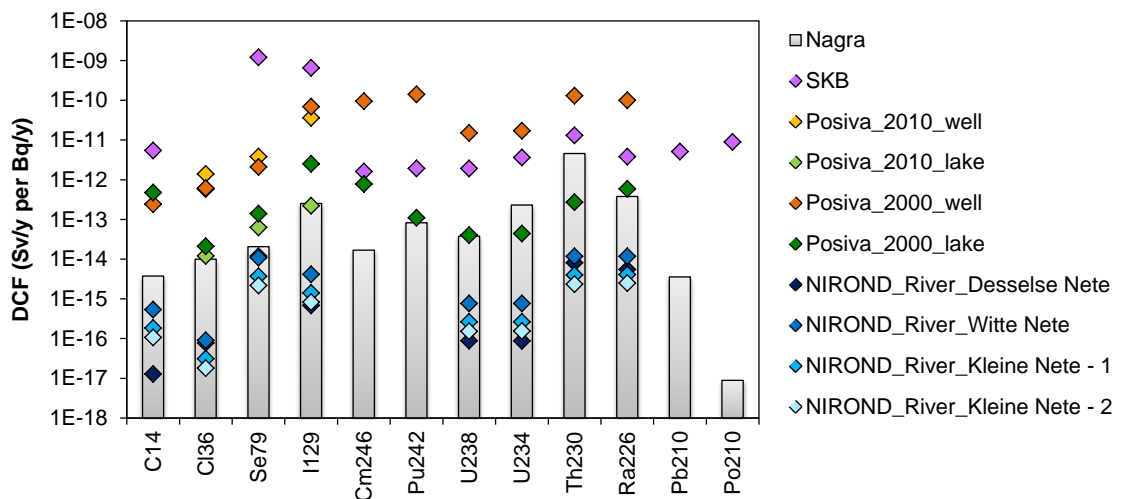


Figure 44: Comparison of BDCF of the present study (grey columns) and the dose conversion factors obtained in different approaches of national radioactive waste management agencies (markers)

Differences observed between approaches are mainly due to the conceptualization of the biosphere model and the parameterization of the required data. In fact, in most cases the conversion factor is calculated for a specific biosphere subsystem and not for the whole biosphere system as it is done in the case of Nagra’s approach. In addition,

almost all models neglect the well scenario and the use of groundwater for agriculture or stockbreeding.

When comparing only with the models considering the well scenario (purple (SKB), yellow (Posiva in 2010) and orange (Posiva in 2000) markers in Figure 44, SKB and Posiva results are higher for all radionuclides. Posiva's model (Figure 32, right side) is based on an influx of contaminated water directly to the well without assuming the dilution effect of the aquifer as it is assumed in Nagra's approach. This may lead to a higher radionuclide concentration in drinking water, foodstuff and soil, thus resulting in a higher dose. SKB developed a more complex model than the one used in Nagra's approach, and the difference between final results may be due to both the model description and the selected data for the required parameters.

7. Summary and Conclusions

The Swiss Federal Nuclear Safety Inspectorate (ENSI) is in charge of reviewing the work developed by the National Cooperative for the Disposal of Radioactive Waste (Nagra) in Switzerland. Within the context of the 'Opalinus Clay' project, the performance and safety assessment exercise developed by Nagra involved the derivation of Biosphere Dose Conversion Factors (BDCF).

The objective of the work reported in this document is the derivation of Biosphere Dose Conversion Factors (BDCF) by using an alternative modeling tool and the study of how several simplifications incorporated to the model can affect the results.

The present work also constitutes the basis of an expanded study aiming at developing ENSI's biosphere modeling capabilities, including the selection of a suitable computer program for biosphere transport and dose calculations alternative to the one used by Nagra.

Along this work, the compartmental code AMBER© has been used to obtain the values of the BDCF, in contrast to the code TAME used in the assessment of Nagra. The results obtained are in agreement with the ones reported by Nagra, which is a confirmation of the validity of the numerical implementation in AMBER©.

The project has been divided into four sections dealing with (1) the description of the conceptual model and its implementation in AMBER©, (2) the comparison exercise between BDCF results obtained by Nagra and the ones derived in this study, (3) sensitivity analyses of the results versus different exposure pathways and contamination paths and (4) the comparison of the BDCF resulting from the reference model with the ones obtained by other biosphere approaches carried out by different national radioactive waste management agencies.

Twelve radionuclides have been included in the analyses: four non-metallic elements (^{14}C , ^{36}Cl , ^{79}Se , ^{129}I) and 8 metallic elements that are part of the decay chain of ^{246}Cm (^{242}Pu , ^{238}U , ^{234}U , ^{230}Th , ^{226}Ra , ^{210}Pb , ^{210}Po).

Results of the present study are in good agreement with the BDFCs presented by Nagra in the context of the 'Opalinus Clay' project.

According to the results, ingestion is the pathway contributing most to the total received dose for an individual of the critical group (these conclusions are valid for the radionuclides and the system under study).

Two general trends can be distinguished between metallic and non-metallic elements when analysing their contribution to the ingestion pathway. Metallic elements present high sorption coefficients, resulting in higher concentration in the top-soil and bed sediments, while non-metallic elements are more concentrated in the local aquifer and surface water. Ingestion of milk provides a good example to study this distinctive behaviour. Soil consumption and pasture consumption contaminated by root uptake are the main mechanisms of milk contamination in the case of metallic elements, while drinking water and consumption of pasture contaminated by irrigation are the ones dominating for non-metallic elements.

The elimination of the solid material fluxes in the model results in calculated BDCF higher than the ones of the reference case, therefore resulting in a conservative approach or simplification.

A comparison has been done between the model implemented and the approaches followed by different radioactive waste management agencies such as SKB, Posiva or Andra. A summary of conclusions obtained in the PAMINA project regarding dose conversion factors and biosphere modelling is also presented. A wide range of DCF values is provided in literature, mainly due to the conceptualization of the biosphere system and the database used for calculations.

The following three aspects of the comparison and sensitivity analyses exercise can be highlighted:

1. The model implemented in TAME by Nagra is absolutely transportable to the AMBER code. The results do not depend on the numerical code used, in this case AMBER© can be used to implement the conceptual model developed for the Opalinus Clay exercise.
2. The sensitivity analyses have shown that ingestion is the main contributor to the dose, and that the exposure pathways through fish and eggs can be neglected in the assessment without jeopardizing the accuracy of the results (always for the radionuclides and for the model treated in this report).

-
3. For most of the metallic radionuclides included in the analyses, BDCFs up to 3 times larger are obtained if solid material fluxes are neglected. This highlights the relevance of properly describing the association of radionuclides with solid material as well as the adequacy of selecting an appropriate set of data to describe solid/radionuclide interactions.

8. References

Albrecht, A., Altmann, S., Buschaert, S., Coelho, D., Gallerand, M.O., Giffaut, E., Leclerc-Cessac, E. (2005) Dossier 2005. Argile Référentiel de comportement des radionucléides et des toxiques chimiques d'un stockage dans le Callovo-Oxfordien jusqu'à l'homme. Site de Meuse/Haute-Marne. Tome 2/2: Chapitres 5 à 7. Andra Report, C.RP.ASTR.04.0032

Albrecht, A. and Miquel, S. (2010) Extension of sensitivity and uncertainty analysis for long term dose assessment of high level nuclear waste disposal sites to uncertainties in the human behavior. J. Environ. Radioact., 101, 55-67

Avila, R., Ekström, P-A., Åstrand, P-G. (2010) Landscape dose conversion factors used in the safety assessment SR-Site. SKB Technical Report, TR-10-06

Ekström, P-A. (2010) Pandora – a simulation tool for safety assessments. Technical description and user's guide. SKB Report, R-11-01

Galson, D.A., Klos, R.A., Serres, C., Mathieu, G., Beuth, T., Cormenazana, J.L. (2009) Task reports for the third group of topics: Biosphere, Human intrusion, Criteria for Input and Data Selection. Deliverable of the PAMINA project, D-Nº:1.1.3

Karlsson, S. and Bergström, U. (2000) Dose rate estimated for the Olkiluoto site using the biosphere models of Sr-97. Posiva Working Report, 2000-20

Klos, R.A., Müller-Lemans, H., van Drop, F., Gribi, P. (1996) TAME – The Terrestrial-Aquatic Model of the Environment: Model Definition. Nagra Technical Report, NTB 93-04

Kyllönen, J. and Keto, V. (2010) Biosphere Analysis – a Complementary Assessment of Dose Conversion Factors for the Olkiluoto Site. Posiva Working Report, 2010-18

Nagra (2002a) Safety Report. Demonstration of disposal feasibility for spent fuel, vitrified high-level waste and long-lived intermediate-level waste (Entsorgungsnachweis). *Project Opalinus Clay*. Nagra Technical Report, NTB 02-05



Nagra (2002b) Models, Codes and Data for Safety Assessment. Demonstration of disposal feasibility for spent fuel, vitrified high-level waste and long-lived intermediate-level waste (Entsorgungsnachweis). *Project Opalinus Clay*. Nagra Technical Report, NTB 02-06

Nagra (2003) Biosphere modelling for the Opalinus Clay safety assessment concepts and data. Nagra Internal Report, NIB 02-01

NIROND (2001) SAFIR 2. Safety Assessment and Feasibility Interim Report 2. ONDRAF/NIRAD Report, NIROND 2001-06 E

NWMO (2011) SYVAC3-CC4 Theory. NWMO Technical Report, TR-2011-20

Quintessa Limited (2011) AMBER 5.5 Reference Guide. QE-AMBER-1, Version 5.5

SKB (2010) Biosphere analyses for the safety assessment SR-Site – synthesis and summary of results. SKB Technical Report, TR-10-09

SKB (2011) Long-term safety for the final repository for spent nuclear fuel at Forsmark. Main report of the SR-Site project. Volume III. SKB Technical Report, TR-11-01

Appendix A: Data used for Reference Case

All data used for BDCF calculations are presented in this appendix and are classified as follows:

1. Specific radionuclide data
2. Non-radionuclide dependent data used in physical sub-model
3. Radionuclide dependent data used in physical sub-model
4. Non-radionuclide dependent data used in exposure pathway sub-model
5. Radionuclide dependent data used in exposure pathway sub-model

A1. Specific radionuclide data

Table 9: Radionuclides of interest in the present study, their daughters and half-life (st = stable isotope)

	Radionuclide	Daughter	Half-life (y)
Non-metallic elements	^{14}C	^{14}N (st)	$5.7 \cdot 10^3$
	^{36}Cl	^{36}Ar (st)	$3.0 \cdot 10^5$
	^{79}Se	^{79}Br (st)	$1.1 \cdot 10^6$
	^{129}I	^{129}Xe (st)	$1.6 \cdot 10^7$
Metallic elements	^{246}Cm	^{242}Pu	$4.7 \cdot 10^3$
	^{242}Pu	^{238}U	$3.8 \cdot 10^5$
	^{238}U	^{234}U	$4.5 \cdot 10^9$
	^{234}U	^{230}Th	$2.5 \cdot 10^5$
	^{230}Th	^{226}Ra	$7.5 \cdot 10^4$
	^{226}Ra	^{210}Pb	$1.6 \cdot 10^3$
	^{210}Pb	^{210}Po	$2.2 \cdot 10^1$
	^{210}Po	^{206}Pb (st)	$3.8 \cdot 10^{-1}$

A2. Non-radionuclide dependent data used in physical sub-model

Table 10: Data selected for parameters used in the development of the physical sum-model which are independent on the radionuclide

	Parameter	Units	Value
Generic data	A_f	m^2	$2.3 \cdot 10^6$
	D_0	m^2/y	0.038
	ETP	m/y	0.6
	$RAINFALL$	m/y	1
	$IRRI_L$	m/y	0.5
	M_e	$kg/(m^2 \cdot y)$	0.27
	α_P	kg/m^3	0.1
Deep soil data	α_D	kg/m^3	0.001
	ε_D	-	0.4
	L_D	m	2
	M_D	kg/m^2	0.1
	ρ_D	kg/m^3	2650
	θ_D	-	0.3
	T_D	-	3.9
	W_D	y^{-1}	20
Local aquifer data	α_L	kg/m^3	0.001
	ε_L	-	0.2
	L_L	m	20
	ρ_L	kg/m^3	2650
	θ_L	-	0.2
	T_L	-	8.6
Surface water data	α_L	kg/m^3	0.1
	D_W	m	3.25
	L_W	m	3500

	Parameter	Units	Value
	ρ_W	kg/m ³	1000
	W_W	m	100
Bed sediments data	ε_S	-	0.5
	κ_{SW}	y ⁻¹	1
	D_S	m	0.1
	ρ_S	kg/m ³	2650
	θ_S	-	0.5
	T_S	-	2.9
Top soil data	α_T	kg/m ³	0.001
	ε_T	-	0.4
	L_T	m	0.25
	ρ_T	kg/m ³	2650
	θ_T	-	0.3
	T_T	-	3.9

Table 11: Water (m³/y) and solid material (m³/y) fluxes and effective diffusion rate (y⁻¹) implemented in the model (calculated as described in section 3.2)

Transference	Flux	Value
Deep soil → Local aquifer	Water	2.1·10 ⁶
	Solid material	1.2·10 ³
	Diffusion	7.3·10 ⁻⁴
Deep soil → Top soil	Solid material	5.2·10 ⁶
	Diffusion	5.8·10 ⁻³
Local aquifer → Deep soil	Solid material	6.2·10 ⁵
	Diffusion	2.2·10 ⁻⁵
Local aquifer → Bed sediments	Water	2.6·10 ⁶
	Solid material	2.6·10 ³
	Diffusion	4.4·10 ⁻⁴
Local aquifer → Top soil	Water	1.2·10 ⁶

Transference	Flux	Value
	Solid material	$1.2 \cdot 10^3$
Bed Sediments → Local aquifer	Diffusion	$6.6 \cdot 10^{-1}$
	Water	$2.6 \cdot 10^6$
Bed Sediments → Surface water	Solid material	$4.6 \cdot 10^7$
	Water	$2.1 \cdot 10^6$
Top soil → Deep soil	Solid material	$4.6 \cdot 10^6$
	Diffusion	$4.7 \cdot 10^{-2}$
Top soil → Surface water	Solid material	$6.2 \cdot 10^5$
	Water	$1.2 \cdot 10^{10}$
Surface water → Elsewhere	Solid material	$1.2 \cdot 10^9$
Surface water → Bed Sediments	Solid material	$4.6 \cdot 10^7$

Table 12: Water fluxes (m^3/y) entering the biosphere system

Flux	Description	Value
F_{CL}	Flux of contaminated deep groundwater into local aquifer	$1.3 \cdot 10^5$
F_{UL}	Flux of uncontaminated deep groundwater into local aquifer	$1.5 \cdot 10^6$
F_{UW}	Flux of uncontaminated water into surface water	$1.2 \cdot 10^{10}$

A3. Radionuclide dependent data used in physical sub-model

Table 13: Sorption coefficients (K_d) expressed in m^3/kg for both types of soil considered in the model

Element	Coarse*	Fine**
C	0.005	0.005
Cl	0	0
Se	0.001	0.01
I	0.0001	0.001
Cm	1	10
Pu	1	10
U	0.1	1
Th	1	10
Ra	0.1	1
Pb	0.1	1
Po	1	10

* Grain size of L and S

** Grain size of D, T and W

Table 14: Radionuclide transfer rates in y^{-1} by advection, solid material transport, diffusion and total transfer rates implemented in the model (calculated as described in section 3.2)

Deep soil → Local aquifer				
<i>Element</i>	<i>Advection</i>	<i>Solid material</i>	<i>Diffusion</i>	<i>Total</i>
C	$5.5 \cdot 10^{-2}$	$1.5 \cdot 10^{-7}$	$8.9 \cdot 10^{-5}$	$5.5 \cdot 10^{-2}$
Cl	$1.5 \cdot 10^0$	$0.0 \cdot 10^0$	$2.4 \cdot 10^{-3}$	$1.5 \cdot 10^0$
Se	$2.8 \cdot 10^{-2}$	$1.5 \cdot 10^{-7}$	$4.5 \cdot 10^{-5}$	$2.8 \cdot 10^{-2}$
I	$2.4 \cdot 10^{-1}$	$1.3 \cdot 10^{-7}$	$3.9 \cdot 10^{-4}$	$2.4 \cdot 10^{-1}$
Cm	$2.8 \cdot 10^{-5}$	$1.6 \cdot 10^{-7}$	$4.6 \cdot 10^{-8}$	$2.8 \cdot 10^{-5}$

Pu	$2.8 \cdot 10^{-5}$	$1.6 \cdot 10^{-7}$	$4.6 \cdot 10^{-8}$	$2.8 \cdot 10^{-5}$
U	$2.8 \cdot 10^{-4}$	$1.6 \cdot 10^{-7}$	$4.6 \cdot 10^{-7}$	$2.8 \cdot 10^{-4}$
Th	$2.8 \cdot 10^{-5}$	$1.6 \cdot 10^{-7}$	$4.6 \cdot 10^{-8}$	$2.8 \cdot 10^{-5}$
Ra	$2.8 \cdot 10^{-4}$	$1.6 \cdot 10^{-7}$	$4.6 \cdot 10^{-7}$	$2.8 \cdot 10^{-4}$
Pb	$2.8 \cdot 10^{-4}$	$1.6 \cdot 10^{-7}$	$4.6 \cdot 10^{-7}$	$2.8 \cdot 10^{-4}$
Po	$2.8 \cdot 10^{-5}$	$1.6 \cdot 10^{-7}$	$4.6 \cdot 10^{-8}$	$2.8 \cdot 10^{-5}$

Deep soil → Top soil

<i>Element</i>	<i>Advection</i>	<i>Solid material</i>	<i>Diffusion</i>	<i>Total</i>
C		$6.9 \cdot 10^{-4}$	$7.1 \cdot 10^{-4}$	$1.4 \cdot 10^{-3}$
Cl		$0.0 \cdot 10^0$	$1.9 \cdot 10^{-2}$	$1.9 \cdot 10^{-2}$
Se		$7.0 \cdot 10^{-4}$	$3.6 \cdot 10^{-4}$	$1.1 \cdot 10^{-3}$
I		$6.0 \cdot 10^{-4}$	$3.1 \cdot 10^{-3}$	$3.7 \cdot 10^{-3}$
Cm		$7.1 \cdot 10^{-4}$	$3.7 \cdot 10^{-7}$	$7.1 \cdot 10^{-4}$
Pu		$7.1 \cdot 10^{-4}$	$3.7 \cdot 10^{-7}$	$7.1 \cdot 10^{-4}$
U		$7.1 \cdot 10^{-4}$	$3.7 \cdot 10^{-6}$	$7.2 \cdot 10^{-4}$
Th		$7.1 \cdot 10^{-4}$	$3.7 \cdot 10^{-7}$	$7.1 \cdot 10^{-4}$
Ra		$7.1 \cdot 10^{-4}$	$3.7 \cdot 10^{-6}$	$7.2 \cdot 10^{-4}$
Pb		$7.1 \cdot 10^{-4}$	$3.7 \cdot 10^{-6}$	$7.2 \cdot 10^{-4}$
Po		$7.1 \cdot 10^{-4}$	$3.7 \cdot 10^{-7}$	$7.1 \cdot 10^{-4}$

Local aquifer → Deep soil

<i>Element</i>	<i>Advection</i>	<i>Solid material</i>	<i>Diffusion</i>	<i>Total</i>
C		$6.3 \cdot 10^{-6}$	$2.0 \cdot 10^{-6}$	$8.3 \cdot 10^{-6}$
Cl		$0.0 \cdot 10^0$	$1.1 \cdot 10^{-4}$	$1.1 \cdot 10^{-4}$
Se		$5.8 \cdot 10^{-6}$	$9.5 \cdot 10^{-6}$	$1.5 \cdot 10^{-5}$
I		$3.3 \cdot 10^{-6}$	$5.4 \cdot 10^{-5}$	$5.7 \cdot 10^{-5}$
Cm		$6.4 \cdot 10^{-6}$	$1.0 \cdot 10^{-8}$	$6.4 \cdot 10^{-6}$
Pu		$6.4 \cdot 10^{-6}$	$1.0 \cdot 10^{-8}$	$6.4 \cdot 10^{-6}$
U		$6.4 \cdot 10^{-6}$	$1.0 \cdot 10^{-7}$	$6.5 \cdot 10^{-6}$
Th		$6.4 \cdot 10^{-6}$	$1.0 \cdot 10^{-8}$	$6.4 \cdot 10^{-6}$
Ra		$6.4 \cdot 10^{-6}$	$1.0 \cdot 10^{-7}$	$6.5 \cdot 10^{-6}$
Pb		$6.4 \cdot 10^{-6}$	$1.0 \cdot 10^{-7}$	$6.5 \cdot 10^{-6}$
Po		$6.4 \cdot 10^{-6}$	$1.0 \cdot 10^{-8}$	$6.4 \cdot 10^{-6}$

Local aquifer → Bed sediments

<i>Element</i>	<i>Advection</i>	<i>Solid material</i>	<i>Diffusion</i>	<i>Total</i>
C	$5.1 \cdot 10^{-3}$	$2.6 \cdot 10^{-8}$	$4.1 \cdot 10^{-5}$	$5.2 \cdot 10^{-3}$
Cl	$2.8 \cdot 10^{-1}$	$0.0 \cdot 10^0$	$2.2 \cdot 10^{-3}$	$2.8 \cdot 10^{-1}$
Se	$2.4 \cdot 10^{-2}$	$2.4 \cdot 10^{-8}$	$1.9 \cdot 10^{-4}$	$2.4 \cdot 10^{-2}$
I	$1.3 \cdot 10^{-1}$	$1.3 \cdot 10^{-8}$	$1.1 \cdot 10^{-3}$	$1.4 \cdot 10^{-1}$
Cm	$2.6 \cdot 10^{-5}$	$2.6 \cdot 10^{-8}$	$2.1 \cdot 10^{-7}$	$2.6 \cdot 10^{-5}$
Pu	$2.6 \cdot 10^{-5}$	$2.6 \cdot 10^{-8}$	$2.1 \cdot 10^{-7}$	$2.6 \cdot 10^{-5}$
U	$2.6 \cdot 10^{-4}$	$2.6 \cdot 10^{-8}$	$2.1 \cdot 10^{-6}$	$2.6 \cdot 10^{-4}$
Th	$2.6 \cdot 10^{-5}$	$2.6 \cdot 10^{-8}$	$2.1 \cdot 10^{-7}$	$2.6 \cdot 10^{-5}$
Ra	$2.6 \cdot 10^{-4}$	$2.6 \cdot 10^{-8}$	$2.1 \cdot 10^{-6}$	$2.6 \cdot 10^{-4}$
Pb	$2.6 \cdot 10^{-4}$	$2.6 \cdot 10^{-8}$	$2.1 \cdot 10^{-6}$	$2.6 \cdot 10^{-4}$
Po	$2.6 \cdot 10^{-5}$	$2.6 \cdot 10^{-8}$	$2.1 \cdot 10^{-7}$	$2.6 \cdot 10^{-5}$

Local aquifer → Top soil

<i>Element</i>	<i>Advection</i>	<i>Solid material</i>	<i>Diffusion</i>	<i>Total</i>
C	$2.3 \cdot 10^{-3}$	$1.2 \cdot 10^{-8}$		$2.3 \cdot 10^{-3}$
Cl	$1.3 \cdot 10^{-1}$	$0.0 \cdot 10^0$		$1.3 \cdot 10^{-1}$
Se	$1.1 \cdot 10^{-2}$	$1.1 \cdot 10^{-8}$		$1.1 \cdot 10^{-2}$
I	$6.1 \cdot 10^{-2}$	$6.1 \cdot 10^{-9}$		$6.1 \cdot 10^{-2}$
Cm	$1.2 \cdot 10^{-5}$	$1.2 \cdot 10^{-8}$		$1.2 \cdot 10^{-5}$
Pu	$1.2 \cdot 10^{-5}$	$1.2 \cdot 10^{-8}$		$1.2 \cdot 10^{-5}$
U	$1.2 \cdot 10^{-4}$	$1.2 \cdot 10^{-8}$		$1.2 \cdot 10^{-4}$
Th	$1.2 \cdot 10^{-5}$	$1.2 \cdot 10^{-8}$		$1.2 \cdot 10^{-5}$
Ra	$1.2 \cdot 10^{-4}$	$1.2 \cdot 10^{-8}$		$1.2 \cdot 10^{-4}$
Pb	$1.2 \cdot 10^{-4}$	$1.2 \cdot 10^{-8}$		$1.2 \cdot 10^{-4}$
Po	$1.2 \cdot 10^{-5}$	$1.2 \cdot 10^{-8}$		$1.2 \cdot 10^{-5}$

Bed sediments → Local aquifer

<i>Element</i>	<i>Advection</i>	<i>Solid material</i>	<i>Diffusion</i>	<i>Total</i>
C			$9.2 \cdot 10^{-2}$	$9.2 \cdot 10^{-2}$
Cl			$1.3 \cdot 10^0$	$1.3 \cdot 10^0$
Se			$3.6 \cdot 10^{-1}$	$3.6 \cdot 10^{-1}$
I			$1.0 \cdot 10^0$	$1.0 \cdot 10^0$

Cm		$4.9 \cdot 10^{-4}$	$4.9 \cdot 10^{-4}$	
Pu		$4.9 \cdot 10^{-4}$	$4.9 \cdot 10^{-4}$	
U		$4.9 \cdot 10^{-3}$	$4.9 \cdot 10^{-3}$	
Th		$4.9 \cdot 10^{-4}$	$4.9 \cdot 10^{-4}$	
Ra		$4.9 \cdot 10^{-3}$	$4.9 \cdot 10^{-3}$	
Pb		$4.9 \cdot 10^{-3}$	$4.9 \cdot 10^{-3}$	
Po		$4.9 \cdot 10^{-4}$	$4.9 \cdot 10^{-4}$	
Bed sediments → Surface water				
<i>Element</i>	<i>Advection</i>	<i>Solid material</i>	<i>Diffusion</i>	<i>Total</i>
C	$1.0 \cdot 10^1$	$9.3 \cdot 10^{-1}$		$1.1 \cdot 10^1$
Cl	$1.5 \cdot 10^2$	$0.0 \cdot 10^0$		$1.5 \cdot 10^2$
Se	$4.0 \cdot 10^1$	$7.3 \cdot 10^{-1}$		$4.1 \cdot 10^1$
I	$1.2 \cdot 10^2$	$2.1 \cdot 10^{-1}$		$1.2 \cdot 10^2$
Cm	$5.5 \cdot 10^{-2}$	$1.0 \cdot 10^0$		$1.1 \cdot 10^0$
Pu	$5.5 \cdot 10^{-2}$	$1.0 \cdot 10^0$		$1.1 \cdot 10^0$
U	$5.5 \cdot 10^{-1}$	$1.0 \cdot 10^0$		$1.5 \cdot 10^0$
Th	$5.5 \cdot 10^{-2}$	$1.0 \cdot 10^0$		$1.1 \cdot 10^0$
Ra	$5.5 \cdot 10^{-1}$	$1.0 \cdot 10^0$		$1.5 \cdot 10^0$
Pb	$5.5 \cdot 10^{-1}$	$1.0 \cdot 10^0$		$1.5 \cdot 10^0$
Po	$5.5 \cdot 10^{-2}$	$1.0 \cdot 10^0$		$1.1 \cdot 10^0$
Top soil → Deep soil				
<i>Element</i>	<i>Advection</i>	<i>Solid material</i>	<i>Diffusion</i>	<i>Total</i>
C	$4.4 \cdot 10^{-1}$	$4.8 \cdot 10^{-3}$	$5.7 \cdot 10^{-3}$	$4.5 \cdot 10^{-1}$
Cl	$1.2 \cdot 10^1$	$0.0 \cdot 10^0$	$1.6 \cdot 10^{-1}$	$1.2 \cdot 10^1$
Se	$2.2 \cdot 10^{-1}$	$4.9 \cdot 10^{-3}$	$2.9 \cdot 10^{-3}$	$2.3 \cdot 10^{-1}$
I	$1.9 \cdot 10^0$	$4.2 \cdot 10^{-3}$	$2.5 \cdot 10^{-2}$	$1.9 \cdot 10^0$
Cm	$2.3 \cdot 10^{-4}$	$5.0 \cdot 10^{-3}$	$2.9 \cdot 10^{-6}$	$5.3 \cdot 10^{-3}$
Pu	$2.3 \cdot 10^{-4}$	$5.0 \cdot 10^{-3}$	$2.9 \cdot 10^{-6}$	$5.3 \cdot 10^{-3}$
U	$2.3 \cdot 10^{-3}$	$5.0 \cdot 10^{-3}$	$2.9 \cdot 10^{-5}$	$7.3 \cdot 10^{-3}$
Th	$2.3 \cdot 10^{-4}$	$5.0 \cdot 10^{-3}$	$2.9 \cdot 10^{-6}$	$5.3 \cdot 10^{-3}$
Ra	$2.3 \cdot 10^{-3}$	$5.0 \cdot 10^{-3}$	$2.9 \cdot 10^{-5}$	$7.3 \cdot 10^{-3}$
Pb	$2.3 \cdot 10^{-3}$	$5.0 \cdot 10^{-3}$	$2.9 \cdot 10^{-5}$	$7.3 \cdot 10^{-3}$

	Po	2.3·10 ⁻⁰⁴	5.0·10 ⁻⁰³	2.9·10 ⁻⁰⁶	5.3·10 ⁻⁰³
Top soil → Surface water					
<i>Element</i>	<i>Advection</i>	<i>Solid material</i>	<i>Diffusion</i>	<i>Total</i>	
C		6.5·10 ⁻⁴		6.5·10 ⁻⁴	
Cl		0.0·10 ⁰		0.0·10 ⁰	
Se		6.7·10 ⁻⁴		6.7·10 ⁻⁴	
I		5.7·10 ⁻⁴		5.7·10 ⁻⁴	
Cm		6.8·10 ⁻⁴		6.8·10 ⁻⁴	
Pu		6.8·10 ⁻⁴		6.8·10 ⁻⁴	
U		6.8·10 ⁻⁴		6.8·10 ⁻⁴	
Th		6.8·10 ⁻⁴		6.8·10 ⁻⁴	
Ra		6.8·10 ⁻⁴		6.8·10 ⁻⁴	
Pb		6.8·10 ⁻⁴		6.8·10 ⁻⁴	
Po		6.8·10 ⁻⁴		6.8·10 ⁻⁴	
Surface water → Elsewhere					
<i>Element</i>	<i>Advection</i>	<i>Solid material</i>	<i>Diffusion</i>	<i>Total</i>	
C	1.1E ⁴	5.3E ⁰		1.1E ⁴	
Cl	1.1E ⁴	0.0E ⁰		1.1E ⁴	
Se	1.1E ⁴	1.1E ¹		1.1E ⁴	
I	1.1E ⁴	1.1E ⁰		1.1E ⁴	
Cm	1.1E ⁴	1.1E ⁴		2.1E ⁴	
Pu	1.1E ⁴	1.1E ⁴		2.1E ⁴	
U	1.1E ⁴	1.1E ³		1.2E ⁴	
Th	1.1E ⁴	1.1E ⁴		2.1E ⁴	
Ra	1.1E ⁴	1.1E ³		1.2E ⁴	
Pb	1.1E ⁴	1.1E ³		1.2E ⁴	
Po	1.1E ⁴	1.1E ⁴		2.1E ⁴	
Surface water → Bed sediments					
<i>Element</i>	<i>Advection</i>	<i>Solid material</i>	<i>Diffusion</i>	<i>Total</i>	
C		2.0E ⁻¹		2.0E ⁻¹	
Cl		0.0E ⁰		0.0E ⁰	
Se		4.1E ⁻¹		4.1E ⁻¹	

I	$4.1E^{-2}$	$4.1E^{-2}$
Cm	$4.1E^2$	$4.1E^2$
Pu	$4.1E^2$	$4.1E^2$
U	$4.1E^1$	$4.1E^1$
Th	$4.1E^2$	$4.1E^2$
Ra	$4.1E^1$	$4.1E^1$
Pb	$4.1E^1$	$4.1E^1$
Po	$4.1E^2$	$4.1E^2$

A4. Non-radionuclide dependent data used in exposure pathway sub-model

Table 15: Data selected for parameters used in the exposure pathway sub-model which are independent of the radionuclide

	Parameter	Units	Value
Human data	E_0	kJ/y	$2.9 \cdot 10^6$
	F_{milk}	-	0.46
	I_{ftuid}	m ³ /y	1.1
	f_{filter}	-	0
	f_{well}	-	1
	F_{egg}	-	0.018
	F_{ff}	-	0.012
	P_{veg}	-	0.72
	P_g	-	0.79
	P_{gv}	-	0.066
	P_{rv}	-	0.15
	P_{fruit}	-	0.045
	I_{air}	m ³ /y	8020
O_f	-	0	
Food data	η_{milk}	kJ/m ³	$2.8 \cdot 10^6$
	η_{egg}	kJ/egg	$3.1 \cdot 10^2$
	η_{ff}	kJ/kg	$5.7 \cdot 10^3$
	η_{gv}	kJ/kg	$1.1 \cdot 10^3$
	η_{rv}	kJ/kg	$3.0 \cdot 10^3$
	η_g	kJ/kg	$1.4 \cdot 10^4$
	η_{meat}	kJ/kg	$8.7 \cdot 10^3$
η_{fruit}	kJ/kg	$2.2 \cdot 10^3$	
Grain data	S_g	kg/kg	$9.0 \cdot 10^{-5}$

	Parameter	Units	Value
	μ_g	m ² /kg	0.66
	Y_g	kg/m ²	0.61
	H_g	y ⁻¹	1
Green vegetables data	S_{gv}	kg/kg	2.0·10 ⁻⁴
	μ_{gv}	m ² /kg	0.14
	Y_{gv}	kg/m ²	3
	H_{gv}	y ⁻¹	2
Root vegetables data	S_{rv}	kg/kg	0
	μ_{rv}	m ² /kg	0.1
	Y_{rv}	kg/m ²	4
	H_{rv}	y ⁻¹	1
Fruit	S_{fruit}	kg/kg	2.5·10 ⁻⁴
	μ_{fruit}	m ² /kg	0.16
	Y_{fruit}	kg/m ²	2.5
	H_{fruit}	y ⁻¹	1
Cattle data	I_{wc}	m ³ /d	0.03
	I_{pc}	kg/d	20
	A_{drink}	-	1
Pasture data	Z	-	5
	S_{cp}	kg/kg	0.1
	μ_p	m ² /kg	0.33
	Y_p	kg/m ²	1.2
Poultry data	I_{wh}	m ³ /d	2·10 ⁻⁴
	I_{gh}	kg/d	0.07
	P_{drink}	-	1
Environment data	A_r	kg/m ³	5·10 ⁻⁸
	A_f	kg/m ³	1·10 ⁻⁵

A5. Radionuclide dependent data used in exposure pathway sub-model

Table 16: Concentration ratios (K_i for fish, grain, green vegetables, pasture and root vegetables) and transfer factors (K_i for meat, milk and eggs)

Element	K_{ff} (Bq/kg)/ (Bq/m ³)	K_g (Bq/kg)/ (Bq/kg)	K_{gv} (Bq/kg)/ (Bq/kg)	K_{meat} (Bq/kg)/ (Bq/d)	K_{milk} (Bq/kg)/ (Bq/d)	K_p (Bq/kg)/ (Bq/kg)	K_{rv} (Bq/kg)/ (Bq/kg)	K_{eggs} (Bq/egg)/ (Bq/d)	K_{fruit} (Bq/kg)/ (Bq/kg)
C	$4.6 \cdot 10^0$	$3.0 \cdot 10^1$	$2.0 \cdot 10^0$	$3.1 \cdot 10^{-2}$	$1.2 \cdot 10^{-2}$	$1.0 \cdot 10^0$	$1.0 \cdot 10^0$	$1.0 \cdot 10^{-1}$	$1.0 \cdot 10^0$
Cl	$1.0 \cdot 10^{-2}$	$4.5 \cdot 10^1$	$5.0 \cdot 10^0$	$8.0 \cdot 10^{-2}$	$5.0 \cdot 10^{-2}$	$1.3 \cdot 10^1$	$7.5 \cdot 10^0$	$1.0 \cdot 10^0$	$7.5 \cdot 10^0$
Se	$2.0 \cdot 10^{-1}$	$3.6 \cdot 10^{-2}$	$3.5 \cdot 10^{-2}$	$3.2 \cdot 10^{-1}$	$4.0 \cdot 10^{-3}$	$2.5 \cdot 10^{-1}$	$3.8 \cdot 10^{-2}$	$4.8 \cdot 10^{-1}$	$5.0 \cdot 10^{-1}$
I	$5.0 \cdot 10^{-2}$	$3.6 \cdot 10^{-1}$	$1.9 \cdot 10^{-2}$	$3.6 \cdot 10^{-3}$	$9.9 \cdot 10^{-3}$	$1.0 \cdot 10^{-1}$	$5.6 \cdot 10^{-3}$	$1.5 \cdot 10^{-1}$	$5.0 \cdot 10^{-2}$
Cm	$2.5 \cdot 10^{-2}$	$1.1 \cdot 10^{-3}$	$2.0 \cdot 10^{-4}$	$2.0 \cdot 10^{-4}$	$5.0 \cdot 10^{-6}$	$5.0 \cdot 10^{-4}$	$3.0 \cdot 10^{-4}$	$4.4 \cdot 10^{-4}$	$3.0 \cdot 10^{-4}$
Pu	$5.0 \cdot 10^{-3}$	$1.8 \cdot 10^{-3}$	$1.4 \cdot 10^{-4}$	$2.0 \cdot 10^{-6}$	$1.0 \cdot 10^{-7}$	$9.5 \cdot 10^{-5}$	$3.0 \cdot 10^{-4}$	$3.9 \cdot 10^{-4}$	$1.0 \cdot 10^{-4}$
U	$2.0 \cdot 10^{-3}$	$1.3 \cdot 10^{-3}$	$3.8 \cdot 10^{-4}$	$3.4 \cdot 10^{-4}$	$3.7 \cdot 10^{-4}$	$9.5 \cdot 10^{-4}$	$5.7 \cdot 10^{-4}$	$5.1 \cdot 10^{-2}$	$1.0 \cdot 10^{-4}$
Th	$3.0 \cdot 10^{-2}$	$7.1 \cdot 10^{-4}$	$3.8 \cdot 10^{-4}$	$2.0 \cdot 10^{-4}$	$5.0 \cdot 10^{-6}$	$9.5 \cdot 10^{-4}$	$5.7 \cdot 10^{-4}$	$5.0 \cdot 10^{-2}$	$5.0 \cdot 10^{-2}$
Ra	$2.5 \cdot 10^{-2}$	$1.4 \cdot 10^{-2}$	$1.6 \cdot 10^{-3}$	$9.0 \cdot 10^{-4}$	$4.0 \cdot 10^{-4}$	$4.0 \cdot 10^{-3}$	$3.0 \cdot 10^{-3}$	$4.6 \cdot 10^{-2}$	$4.0 \cdot 10^{-2}$
Pb	$1.0 \cdot 10^{-1}$	$1.7 \cdot 10^{-2}$	$1.8 \cdot 10^{-3}$	$4.0 \cdot 10^{-4}$	$2.6 \cdot 10^{-4}$	$4.5 \cdot 10^{-3}$	$2.7 \cdot 10^{-3}$	$4.6 \cdot 10^{-2}$	$1.0 \cdot 10^{-2}$
Po	$5.0 \cdot 10^{-1}$	$2.0 \cdot 10^{-4}$	$2.0 \cdot 10^{-4}$	$4.0 \cdot 10^{-3}$	$3.0 \cdot 10^{-4}$	$2.0 \cdot 10^{-4}$	$2.0 \cdot 10^{-4}$	$5.0 \cdot 10^{-5}$	$2.0 \cdot 10^{-4}$



Table 17: Food processing retention factors (F_i) and weathering rates (W_i)

Element	F_g	W_g	W_p	F_{gv}	W_{gv}	F_{rv}	W_{rv}	T_{rv}	T_{fruit}
	-	y^{-1}	y^{-1}	-	y^{-1}	-	y^{-1}	y^{-1}	y^{-1}
C	0.15	8.4	18	0.5	18	0.5	18	18000	18000
Cl	0.15	8.4	18	0.5	18	0.5	18	2.0	2.0
Se	0.15	8.4	18	0.5	18	0.5	18	2.02	0.12
I	0.5	8.4	18	0.5	18	0.5	18	2.0	0.33
Cm	0.15	8.4	18	0.5	18	0.5	18	0	0
Pu	0.1	51	18	0.5	51	0.5	18	0	0.19
U	0.15	8.4	18	0.5	18	0.5	18	0.18	0.19
Th	0.15	8.4	18	0.5	18	0.5	18	0.18	0.13
Ra	0.15	8.4	18	0.5	18	0.5	18	0.18	0.073
Pb	0.15	8.4	18	0.5	18	0.5	18	0	0.11
Po	0.15	8.4	18	0.5	18	0.5	18	0.18	0.11



Table 18: Dose coefficients for ingestion (D_{ing}), inhalation (D_{inh}) and external exposure from radionuclides in soil (G)

Element	D_{ing} Sv/Bq	D_{inh} Sv/Bq	G (Sv/y)/ (Bq/m ³)
¹⁴ C	$5.8 \cdot 10^{-10}$	$5.8 \cdot 10^{-9}$	0
³⁶ Cl	$9.3 \cdot 10^{-10}$	$7.3 \cdot 10^{-9}$	0
⁷⁹ Se	$2.9 \cdot 10^{-9}$	$6.8 \cdot 10^{-9}$	0
¹²⁹ I	$1.1 \cdot 10^{-7}$	$3.6 \cdot 10^{-8}$	$3.1 \cdot 10^{-12}$
²⁴⁶ Cm	$2.1 \cdot 10^{-7}$	$9.8 \cdot 10^{-5}$	0
²⁴² Pu	$2.4 \cdot 10^{-7}$	$1.1 \cdot 10^{-4}$	0
²³⁸ U	$4.8 \cdot 10^{-8}$	$8.0 \cdot 10^{-6}$	0
²³⁴ U	$4.9 \cdot 10^{-8}$	$9.4 \cdot 10^{-6}$	$2.7 \cdot 10^{-13}$
²³⁰ Th	$2.1 \cdot 10^{-7}$	$1.0 \cdot 10^{-4}$	$3.0 \cdot 10^{-13}$
²²⁶ Ra	$2.8 \cdot 10^{-7}$	$9.5 \cdot 10^{-6}$	$5.5 \cdot 10^{-12}$
²¹⁰ Pb	$6.9 \cdot 10^{-7}$	$5.7 \cdot 10^{-6}$	$6.2 \cdot 10^{-13}$
²¹⁰ Po	$1.2 \cdot 10^{-6}$	$4.3 \cdot 10^{-6}$	$5.5 \cdot 10^{-14}$

ENSI 33/219

ENSI, CH-5200 Brugg, Industriestrasse 19, Telefon +41 (0)56 460 84 00, E-Mail Info@ensi.ch, www.ensi.ch